

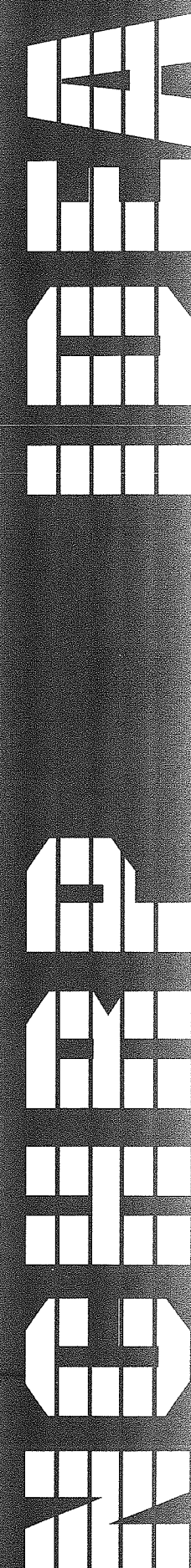
TRANSPORTATION RESEARCH BOARD
NATIONAL RESEARCH COUNCIL



NATIONAL COOPERATIVE HIGHWAY RESEARCH PROGRAM



Report of Investigation



IDEA PROJECT FINAL REPORT
Contract NCHRP-93-ID011

IDEA Program
Transportation Research Board
National Research Council

June 1996

**REHABILITATION OF STEEL BRIDGE
GIRDERS THROUGH THE
APPLICATION OF ADVANCED
COMPOSITE MATERIALS**

Prepared by:
Dennis R. Mertz and John W. Gillespie, Jr.
University of Delaware

**INNOVATIONS DESERVING EXPLORATORY ANALYSIS (IDEA)
PROGRAMS
MANAGED BY THE TRANSPORTATION RESEARCH BOARD (TRB)**

This NCHRP-IDEA investigation was completed as part of the National Cooperative Highway Research Program (NCHRP). The NCHRP-IDEA program is one of the four IDEA programs managed by the Transportation Research Board (TRB) to foster innovations in highway and intermodal surface transportation systems. The other three IDEA program areas are Transit-IDEA, which focuses on products and results for transit practice, in support of the Transit Cooperative Research Program (TCRP), Safety-IDEA, which focuses on motor carrier safety practice, in support of the Federal Motor Carrier Safety Administration and Federal Railroad Administration, and High Speed Rail-IDEA (HSR), which focuses on products and results for high speed rail practice, in support of the Federal Railroad Administration. The four IDEA program areas are integrated to promote the development and testing of nontraditional and innovative concepts, methods, and technologies for surface transportation systems.

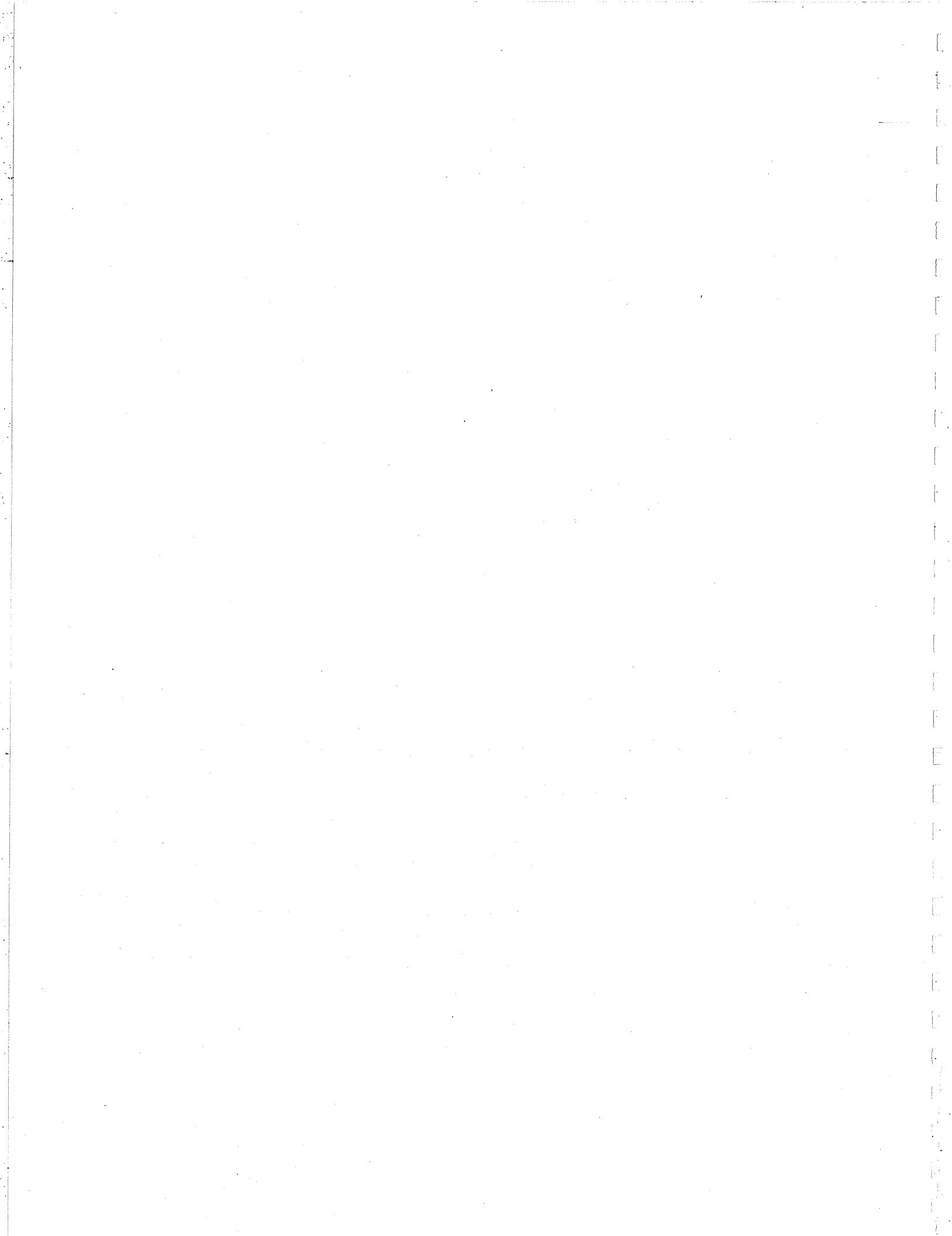
For information on the IDEA Program contact IDEA Program, Transportation Research Board, 500 5th Street, N.W., Washington, D.C. 20001 (phone: 202/334-1461, fax: 202/334-3471, <http://www.nationalacademies.org/trb/idea>)

The project that is the subject of this contractor-authored report was a part of the Innovations Deserving Exploratory Analysis (IDEA) Programs, which are managed by the Transportation Research Board (TRB) with the approval of the Governing Board of the National Research Council. The members of the oversight committee that monitored the project and reviewed the report were chosen for their special competencies and with regard for appropriate balance. The views expressed in this report are those of the contractor who conducted the investigation documented in this report and do not necessarily reflect those of the Transportation Research Board, the National Research Council, or the sponsors of the IDEA Programs. This document has not been edited by TRB.

The Transportation Research Board of the National Academies, the National Research Council, and the organizations that sponsor the IDEA Programs do not endorse products or manufacturers. Trade or manufacturers' names appear herein solely because they are considered essential to the object of the investigation.

TABLE OF CONTENTS

EXECUTIVE SUMMARY	1
PROBLEM STATEMENT	1
RESEARCH APPROACH	1
ADHESIVE DURABILITY TESTING	2
REPAIR AND TESTING OF SCALE GIRDERS.....	4
Repair Schemes	4
Service Load Testing.....	5
<i>Test Setup.....</i>	5
<i>Test Procedure.....</i>	5
<i>Test Results</i>	5
Strength Tests	6
<i>Test Setup.....</i>	6
<i>Test Procedure.....</i>	6
<i>Test Results</i>	6
REPAIR AND TESTING OF FULL-SCALE CORRODED GIRDERS	7
Description of Corroded Bridge Girders	7
Pre-Repair Elastic Testing.....	7
Evaluation of Corroded Bridge Girders.....	7
Steel Section and Material Properties	8
Rehabilitation Procedure.....	8
Post-Repair Ultimate Testing.....	13
<i>Test Setup.....</i>	13
<i>Instrumentation.....</i>	14
<i>Test Procedure.....</i>	14
<i>Test Results</i>	14
Simplified Analysis Method.....	22
<i>Analytical Method.....</i>	22
<i>Correlative Analysis.....</i>	22
<i>Analytical Evaluations for Repair Effectiveness</i>	22
CONCLUSIONS	24
APPENDIX A	26



EXECUTIVE SUMMARY

The objective of this project is to demonstrate the advantages of using advanced composite materials in the rehabilitation of deteriorated steel bridge members. The primary cause of such deterioration is loss of steel due to corrosion. Due to various conditions that accelerate corrosion, such as debris accumulation, the bottom flanges of girders are usually the site of the largest corrosion. The flexural characteristics of steel bridge girders are shown to be improved through the application of various repair schemes to the bottom flange. This investigation has focused on the case of single span girders where the bottom flange is subjected to tensile stresses. The composite rehabilitations are attached to the corroded steel member using adhesive bonding; therefore, the durability of the adhesive bond under the various conditions that are present in the field over time is a critical issue. Durability tests were performed on a number of adhesives to determine the effect of the environmental conditions on the fracture toughness of the bond over time. Rehabilitation schemes were developed and tested for a variety of field conditions. One of the schemes was used to rehabilitate girders taken out of service in Pennsylvania due to excessive corrosion. This provided an opportunity for the process to be applied to a member of realistic size and with corrosion as exists in the national bridge inventory.

PROBLEM STATEMENT

The national bridge inventory is in need of inexpensive measures to extend the life of deteriorated bridges at a minimum inconvenience to the public. The use of composite materials to rehabilitate corroded steel girders has the potential for cost savings and rapid rehabilitation. This project has focused on the viability and feasibility of repairing girder-type members, which have been determined to have less than the desired flexural strength or stiffness; typically this would be due to corrosion of the flange section. Due to the extreme light weight of composite materials and to adhesive or fusion bonding methods, installation of composite rehabilitation will be much faster than the conventional method of steel girder rehabilitation. Typically, installation of heavy steel plates requires holes to be drilled into the beam flange for bolted attachment. Erection of temporary scaffolding is either unnecessary or less extensive for the lighter composite material plates. For a desired stiffness, a carbon composite plate would weight approximately one-tenth the weight of a plate fabricated from steel. A more important issue in bridge repairs than direct costs is the degree to which traffic using the bridge is delayed; because composite materials can be installed more quickly and easily than steel, this delay is reduced. The susceptibility of steel bridge members to chemical reaction with the environment (corrosion) is considered the primary cause of girder deterioration. Due to their low chemical reactivity, composite materials do not suffer from this problem and a rehabilitation performed with composite materials would be less susceptible to future corrosion. Due to their flexible nature, composite retrofits can be tailored to various field conditions such as over-extensively corroded members or riveted members.

Composite materials can be directly bonded to the surface being rehabilitated, eliminating the need for labor-intensive mechanical attachment. Adhesive bonding is achieved using a thermoset epoxy between the steel and the composite. Fusion bonding utilizes a thermoplastic material that is melted in the bonding process; this material can be the matrix material of the composite patch or another compatible bonding interlayer. Vinyl esters can be used with composite fabrics in a resin infusion process. Also, a quick mechanical connection using self-tapping screws was investigated to facilitate composite-to-steel assembly and consolidation pressure during the bonding operation. The use of elevated temperatures in the field to accelerate adhesive cure time or facilitate fusion bonding was investigated using induction and resistance heating units suitable for field implementation.

RESEARCH APPROACH

The two major issues in the use of composites to rehabilitate steel girders are the effectiveness of the repair and its durability. The first issue has been addressed through predictive modeling and experimentation on reinforced sections of two size scales. The second issue concerns the durability of the attachment of the composites to the steel; a selection process for adhesives that demonstrate durability under a variety of anticipated field conditions has been conducted.

ADHESIVE DURABILITY TESTING

Different bonding agents are required for the different rehabilitation schemes. The retrofit schemes involving the attachment of a composite patch to the tension flange of the steel can use thermoset or thermoplastics as adhesives. The retrofit scheme for irregular surfaces requires that a vinyl ester be used, as it can infuse the composite fabric draped over the surface. Previous work has been performed in this area at the Center for Composite Materials at the University of Delaware for selection of a thermoset/thermoplastic adhesive with excellent strength and durability properties by Bourban; this work was expanded with emphasis on steel bridge rehabilitation application. In addition to strength and durability, other processing parameters that would impact field implementation such as pot-life, viscosity, and cure time were considered. The following adhesives were screened:

Thermosets (Prefabricated composite panels, wet lay-up, sandwich construction)

- a) Ciba Geigy AV 8113, AV 8531
- b) Lord Fusor Epoxy
- c) Cytech FM 300
- d) Hysol EA 9394
- e) Ciba-Geigy AV 119

Thermoplastics (Prefabricated composite panels)

- a) PSU
- b) PEEK

Vinyl esters (Resin infusion)

- a) Dow Derakane 411-C50
- b) Dow Derakane 8084

The primary concern is the strength of the bond after curing. The greatest bond strength achieved to date is obtained by fusion bonding thermoplastics. Using only grit blasting for surface treatment, lap-shear strengths of 10 MPa (1450 psi) are achievable. The silane coupling agent (adhesion promoter 6106) was very effective in improving the adhesion at the steel-polymer interface and durability. This is seen in the lap-shear strength value increase to about 27 MPa (3915 psi) for PSU and PEEK. Vinyl esters are used in applications such as the previously mentioned infusion into a composite material wrap. With grit blasting, these specimens show an average lap-shear strength of 15 MPa (2175 psi). Specimens with Kevlar pulp mixed in with the vinyl ester display slightly higher strengths. Thermoset tests have been performed with sand blast and sand blast with silane 6040 surface pre-treatments, including lap-shear specimens of the aforementioned epoxies and epoxies Hysol EA 9394 and Cytech FM 300.

The durability of the various adhesives was tested under different weathering conditions through immersion in hot water at 65°C and 85°C, and deicing solutions (salt water and Cryotech CF 7, a non-chloride deicing agent intended for use in Delaware). The ASTM wedge crack test was used. Figure 1 shows results of bond durability tests in terms of Mode I fracture toughness under saturated conditions. The high-temperature water tests are performed to obtain durability information in a short period of time by accelerating diffusion of solutions into the crack tip. In Figure 1, typical data collected from the wedge test is presented for immersion times exceeding 2 months. Crack growth is monitored until arrest occurs at saturated condition. Given the specimen geometry, crack opening displacement and equilibrium crack length, the fracture toughness is calculated. It is seen that silane-treated joints bonded with PSU show enhanced durability under hot-wet conditions. The silane used here is the Adhesion Promoter 6106. At 65°C, it was seen that the joints bonded with epoxy AV 8113 has a marginally better durability than the other epoxies. It is seen that the silane coupling agent 6040 does not enhance bond durability properties in the AV 8113 and AV 8531 bonded joints. In the Fusor-bonded joints, the silane improves durability of the joint in hot water. At 85°C, loss of bond toughness and crack propagation was very rapid, and no meaningful observations could be made in any of the cases.

Immersion in deicing agents is performed to determine the durability of the composite retrofit under the conditions that degraded the steel. Durability tests in 10% NaCl solution of the epoxies AV 8113 and AV 8531 reveal that the silane treated steel joints are more durable than the sand-blasted joints. For testing in Cryotech CF7, the silane-treated

samples showed marginal improvement in toughness and durability. It can be concluded from these studies that silane treatment of the steel surface improves durability in these environments.

For a thermoset adhesive to retain its strength, it must not be subjected to a service temperature greater than its glass transition temperature. The highest temperature to which bridge members are expected to be subjected is estimated as 60°C. Differential scanning calorimetry (DSC) and dynamic mechanical analysis (DMA) runs to evaluate the glass transition temperatures after prolonged immersion in 65°C have shown that vinyl ester is acceptable.

It is also noteworthy that elevated temperature processing can reduce bonding times for thermosets from 24 hours to the same time-scale as thermoplastics (approximately 10 minutes).

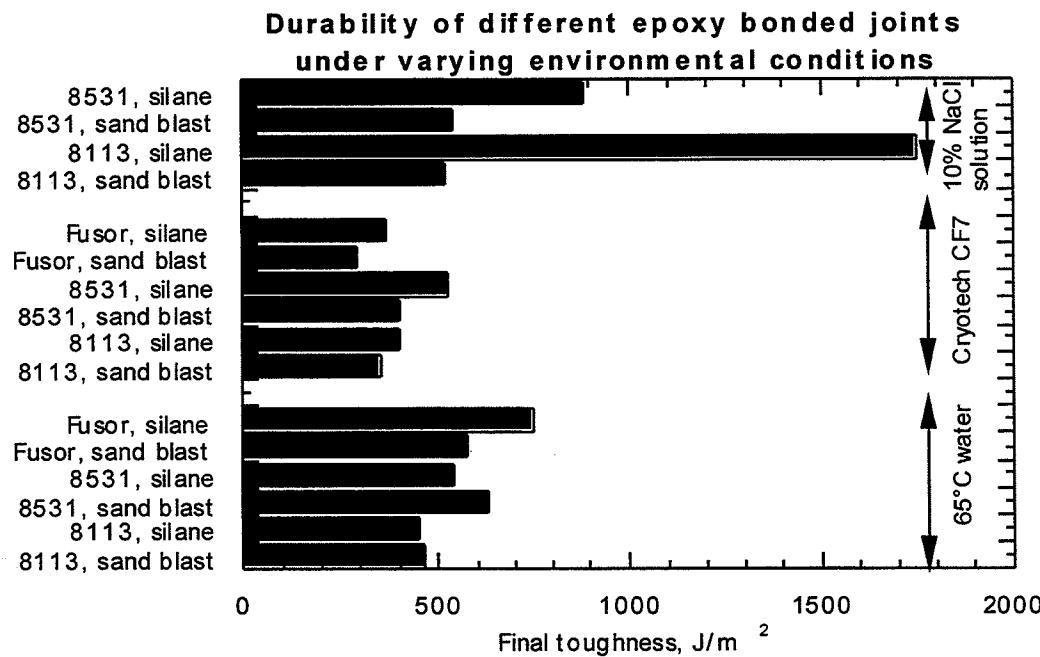


FIGURE 1 Durability of epoxy-bonded joints.

Strength and durability evaluations carried out to date on various epoxy adhesives and vinyl-ester resins have narrowed the adhesive choices to one epoxy adhesive for small- to medium-scale applications—AV 8113. This epoxy is a two-component, Ciba Geigy commercial-grade adhesive with a curing cycle of 20 minutes at 100°C (16-20 hours at room temperature). Other two-component epoxies evaluated were Lord Fusor, Hysol EA9394, and Ciba Geigy AV 8531. Among the epoxy film adhesives tested were Cytec FM300 and FM 235 and Ciba Geigy AV 119. Adhesives were rejected largely due to their poor durability in one/all environments. Another crucial factor to consider is the pot life of the mixed adhesive: epoxies with pot-life in the 25-30 minute range (e.g., AV 8113) were preferred, while low pot-life adhesives (<10 minutes) were rejected. Pot life can be extended if elevated temperature processing is used (e.g., the epoxy film adhesive Cytec FM300 and all of the thermoplastics). The leading adhesive candidates for the PennDOT girders from those tested were AV 8113, AV 119, and FM 235. AV 8113 was chosen for the rehabilitation.

Adhesively-bonded AV 8113 steel joints show very good durability in the three environments tested—65°C water, a commercial deicing solution, and freeze conditions. Also freeze-thaw test data show that the joints are durable under a thermally fatiguing environment. An additional vital consideration is that of a silane surface pretreatment, since it is needed for survival in most of the environments. Incorporation of an epoxy-tailored silane at the steel surface enhances durability and also leads to a greater final fracture toughness (lower final crack length at arrest) over a sand-blast treatment. A quick recount of the durability statistics of AV 8113 bonded joints in the three environments are as follows: over 8 months (6000 hours) in 65°C water and commercial non-chloride deicing conditions, and over 1 month (720 hours=60 12-hour cycles) under thermal fatigue conditions (listed below). Lap-shear strength values for this epoxy are about 12.5 MPa (1800 psi).

REPAIR AND TESTING OF SCALE GIRDERS

Repair Schemes

The base member used in evaluating reinforcement schemes was a W8x10 beam of A709 grade 36 steel. The length of the beam was 1524 mm (60 in.). This member was chosen as a lower bound on the type of members that can be found in use on bridges; its dimensions are proportionally similar to those of steel beams typically used as large primary girders. The reinforcement schemes developed are designed to improve the flexural characteristics of steel girder shapes. A schematic of the four basic reinforcement schemes geometries is shown in Figure 2 and a photograph is shown in Figure 3.

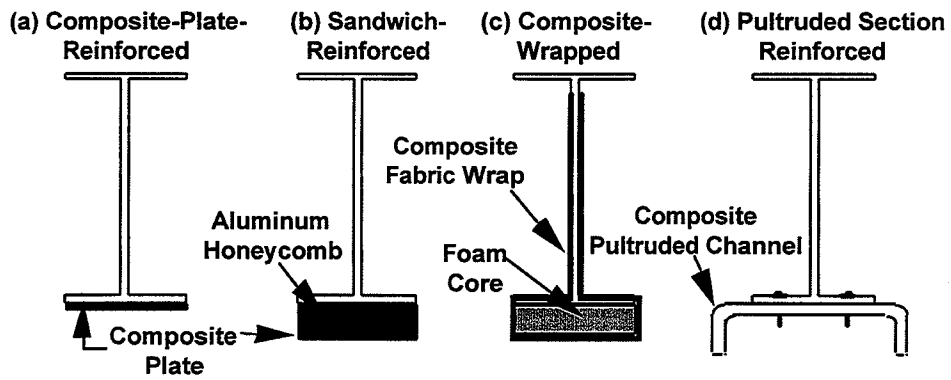


FIGURE 2 Rehabilitation geometries.

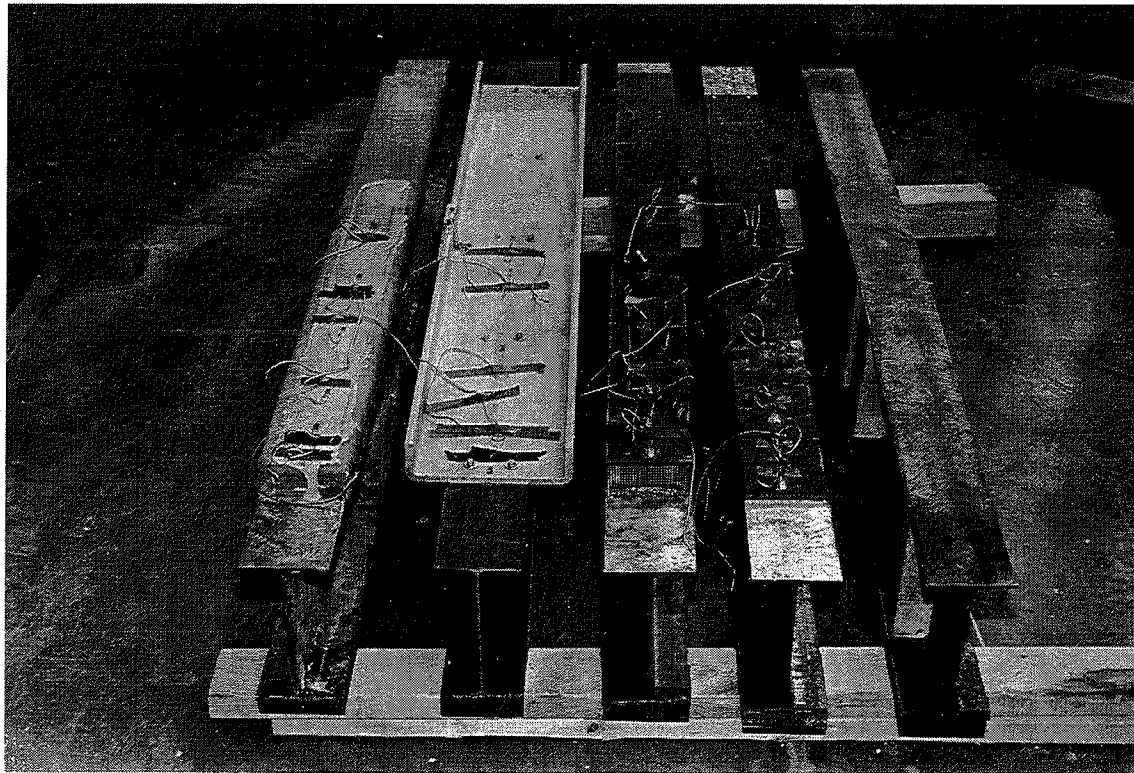


FIGURE 3 Photograph of basic rehabilitation geometries.

The first reinforcement scheme (Figure 2a) was a unidirectional carbon-fiber (IM-7)/epoxy (8551-7) composite plate bonded directly to the tension flange of a beam using a two-part epoxy adhesive (AV8113). The fabricated laminate had a nominal fiber volume fraction of 62%. Two beams of this type were fabricated. The second reinforcement scheme (Figure 2b) used the same composite plate but took advantage of an aluminum honeycomb structure to space the composite plate farther away from the steel section; this forms a composite material system referred to as sandwich construction, where two materials are separated by a core that has practically no influence on the flexural behavior. In these two cases, the thickness of the composite was 4.6 mm (0.18 in), which is comparable to the flange thickness of the base member of 5.1 mm (0.2 in). A different strategy (Figure 2c) was developed for cases where a variable surface might be present, such as due to riveted construction, where a rigid composite member could not be employed. A composite fabric was wrapped from a uniform section on the web of the beam down over the flange and a foam core spacer and up onto the web on the other side. The fabric was a ± 45 degree E-Glass. Three beams of this type were fabricated with differences in the bonding method. The process differed in that a thin layer of epoxy was applied to the steel for the second and third beams and the first layer of fabric was placed over that epoxy before wrapping the subsequent layers. The wrapped sections were then infused with a vinyl ester resin (8084) and vacuum-bagged for curing. The fourth scheme (Figure 2d) utilized an E-Glass pultruded channel adhesively bonded and mechanically connected with self-tapping screws. The fifth scheme is geometrically similar to the first. Three discrete adhesively-bonded pultruded carbon fiber/vinyl ester matrix strips were attached to the tension flange. The strips were 6.4 mm (0.25 in.) thick and 38.1 mm (1.5 in.) wide.

Service Load Testing

Each specimen was tested in the elastic range of the steel to determine the increase in stiffness achieved with the composite reinforcement.

Test Setup

The test setup utilized a 222 kN (50,000 lb.) capacity actuator to apply force through a pivoting fixture that split the force into two applied loads on the beam. The beams had a total length of 1524 mm (60 in.). The composite reinforcement was applied over the central 1219 mm (48 in.) of each beam. The beam was supported 76.2 mm (3 in.) in from each end giving a total span of 1372 mm (54 in.). The applied loads were 203 mm (8 in.) apart symmetric about the center. Hardwood blocks were used at the supports and at the applied loads on both sides of the web to prevent web crippling at the concentrated loads. Strain was measured with bonded strain gages incorporated into quarter Wheatstone bridge configurations with the data acquisition system. Gages were placed at various distances along the half span on the composite materials, and at the midpoint on the interior and exterior of the steel compression flange, the interior steel tension flange (except in the fabric wrapped beams where it was measured on the fabric over the interior of the tension flange), and the exterior on the composite material in tension. Applied load was measured from a voltage generated by a load cell in the actuator. Displacements were measured at the applied force by a LVDT built into the actuator and at desired locations on the beam by DCDTs connected to the data acquisition system. Mid-span deflection was measured in all tests to provide a means of measuring and comparing beam stiffness.

Test Procedure

Testing was performed using a controlled rate of displacement of the actuator head with a 222 kN (50 kip) actuator. Each specimen was cycled five times up to the target load of 89 kN (20 kip) and back to 4.4 kN (1 kip) so that damage to the composites or loss of bond could be observed in the load vs. deflection plots.

Test Results

The service load tests have demonstrated that increases in stiffness can be achieved by using adhesively-bonded composite material plates. The experimentally determined stiffness of each reinforced beam are shown in Table 1.

TABLE 1 Elastic Stiffness Increases

Section	Midspan Stiffness, P/Δ (kN/mm)	Increase Over Control
control beam	43.78	
(a) composite-plated	52.54	20 %
(b) sandwich-reinforced	56.92	30 %
(c) composite-wrapped	48.51	11 %
(d) channel pultrusion-reinforced	53.94	23 %
(e) strip pultrusion-reinforced	55.52	27 %

The different bonding methods for the composite-fabric-reinforced section were found to be critical in the service load tests. The section where the fabric was directly placed on the steel displayed a degradation in stiffness over the four cycles described in the procedure. This indicated that the bond between the steel and composite was breaking. The section which used an initial epoxy adhesive layer displayed no stiffness degradation. All the other sections showed no loss of stiffness with cycling. The tests demonstrated that the steel member can be effectively reinforced with composite material strategies. The differences in stiffness do not reflect differences between the capacity of reinforcement strategies since the material properties and geometries could be tailored to meet any desired stiffness increase. The purpose of the tests was to show that accurately predictable increases could be obtained.

The stiffness increases closely matched the predictions by finite element modeling. All finite element modeling was done with Patran/ABAQUS. Symmetry was used to model half of each member. The stiffness increases based on beam theory with transformed areas and assuming perfect bond also closely match the experimental results for the rigid composite reinforced sections but not for the composite fabric-wrapped section. The fabric-wrapped section demonstrated a nonlinear elastic response.

Strength Tests

Test Setup

The strength test setup was the same as the setup used in the service load tests. The sections were modified by attaching a steel cover plate to the compression flange with an adhesive and bolts. This modification was made to prevent the lateral torsional failure mode of the member. Additionally, this condition better simulates the condition of a girder acting compositely with a concrete deck.

Test Procedure

The beams were monotonically loaded using a 890 kN (200 kip) universal testing machine under pseudo-load control. Displacement, load, and strain were monitored as in the service load tests. The members were loaded beyond the elastic strength until some type of failure occurred where the load-carrying capacity of the member was largely decreased.

Test Results

The strength of the members was defined as the load (or the moment) carried by the section when the tension flange steel reached its yield strain. This value was monitored by a strain gage on the interior of the tension flange for each beam. The strength of each section is shown in Table 2.

TABLE 2 Elastic Strength Increases

Section	Load (kN)	Increase Over Control
control	189	
(a) composite-plated	267	42 %
(b) sandwich-reinforced	323	71 %
(c) composite-wrapped	267	41 %
(d) channel pultrusion-reinforced	259	37 %
(e) strip pultrusion-reinforced	312	65 %

The tests were continued past the defined strengths of the sections to their ultimate failures; the failure load of each specimen is given in Table 3. Specimen *a* failed due to the cover plate debonding from the section at a larger load than the strength of the section. Specimens *b*, *d*, and *e* failed by debonding of the composite reinforcement at an end from the steel flange. Specimen *b* failed before the tension steel reached yield. Specimens *d* and *e* failed at loads significantly greater than the strength of the sections. These bond failures could be forced to higher loads by decreasing the section of the composite toward the ends (tapering) or providing mechanical fasteners if it were desirable to have the ultimate failure load of the specimen be much greater than the strength of the section. Specimen *c* underwent multiple local failures which progressively decreased the section stiffness. The system recovered load after each drop due to a local failure, the section finally failed with the steel cover plate debonding from the compression flange and splits appearing in the E-glass on the web and top flange originating at bolted connections to the cover plate.

TABLE 3 Ultimate Load Capacity.

Section	Load (kN)
(a) composite-plated	323*
(b) sandwich-reinforced	323
(c) composite-wrapped	507
(d) channel pultrusion-reinforced	475
(e) strip pultrusion-reinforced	496

* no failure of the composite system

REPAIR AND TESTING OF FULL-SCALE CORRODED GIRDERS

Description of Corroded Bridge Girders

Full-scale experimentation was carried out to verify the effectiveness of the composite repair system. With the help of PennDOT, arrangements were made to procure four steel girders from a highway bridge that was demolished in August, 1995. Constructed circa 1940 in Valley View, Pennsylvania in western Schuylkill county, the bridge spanned approximately 9754 mm (32 ft.) over Rausch Creek. The deterioration of the girders had progressed to such a point that the bridge had to be temporarily shored at midspan with wooden braces prior to demolition. Corrosion of the steel sections was severe enough on the flanges to warrant the demolition of the bridge. Unfortunately, drawings of the bridge as well as detailed information about the bridge were not available.

Pre-Repair Elastic Testing

The four girders were delivered to Fritz laboratory at Lehigh University in late August, 1995. The first stage of the experimentation consisted of conducting elastic stiffness tests on each girder. The test span was 9144 mm (30 ft.), and the tests were run under three-point loading in the 22,240 kN (5 million lbs.) Baldwin universal testing machine. The instrumentation used was minimal, consisting only of displacement sensors spaced every 1524 mm (60 in.). The girders were then delivered to the University of Delaware.

Since the webs of the girders were not severely corroded, only the bottom flanges were sandblasted. An unusual web splice detail existed near the third point of each girder. The webs were overlapped approximately 305 mm (12 in.) and then fillet welded all around. It was felt that this would have had an adverse effect on the test results and so the girders were cut to eliminate the splice. The elastic stiffness tests were repeated at the University of Delaware with a span of 6401 mm (21 ft.).

Evaluation of Corroded Bridge Girders

The corrosion losses to the girders varied between girders; however, each girder had fairly uniform corrosion along its length. The corrosion was mostly concentrated on the tension flange. An important step with these girders was to determine whether current field evaluation practices could serve as accurate input to the design of a retrofit utilizing composites. A bridge inspector from DelDOT evaluated the condition of the girders in the University of Delaware structures lab in an approximation of the manner in which they would be evaluated in the field. The condition of the girders as would be

recorded in the *PONTIS* bridge management system was determined for each girder. The evaluation of each girder and its experimentally determined stiffness loss is shown in Table 4.

TABLE 4 Comparison Between Field Evaluation and Experimental Data

Girder Number	<i>PONTIS</i> Condition	Experimental Stiffness Loss
1	4	32%
2	3	20%
3	5	24%
4	5	25%

Girders evaluated as being *PONTIS* condition 5 require evaluation by the DOT. The bridge inspector evaluates the corrosion losses and reports the section losses in the inspection report. The DelDOT inspector determined that both of these condition 5 girders had approximately 40% loss of the tension flange. This flange loss corresponds to a stiffness loss of 29%. A comparison of the field evaluation and the experimental stiffness loss show that the current inspection methods may be acceptable for design inputs.

Steel Section and Material Properties

The original section properties of the girders were determined using a historical record of rolled shapes published by AISC. They are summarized in Figure 4. Each girder was 610 mm (24 in.) deep with a 229 mm (9 in.) flange width. Note that the section shape is similar to the American standard I shape with the tapered flanges. These section properties served as the basis for the stiffness comparison in addition to being used to determine the strength using finite element analysis and the approximate method developed.

Judging by the date of construction, the steel used was most likely ASTM A7-39 structural steel. The yield stress is specified as being not less than 228 MPa (33 ksi). Tensile coupon tests were performed to determine the actual yield and ultimate stresses. Two coupons were taken from both the flange and web of each girder. The results are given in Table 5.

TABLE 5 Material Properties of Test Girders

		F_y (MPa)	F_u (MPa)
Girder #1	Flange	283	446
	Web	321	460
Girder #2	Flange	272	439
	Web	307	443

Rehabilitation Procedure

Note that only two of the original four girders were rehabilitated and subsequently tested to failure. The other two girders are to be used for future research involving the effect of a composite slab and fatigue loading.

The four girders each had a splice located at somewhat less than one-third of the span length. The splice was such that the flanges and webs of two girders had been cut so that when the members were joined the webs overlapped each other by one foot and the end of each web was welded to the side of the other web, the flanges were butted together and were welded across that interface. It was decided that the splice in the girders would complicate the analysis and rehabilitation undesirably. Therefore, the first two 9144 mm length girders were cut to remove the spliced section resulting in shorter span girders. The span length for testing was chosen to be 6400.8 mm (21 ft.). In a field rehabilitation it will not be possible to place composites under the section of the girder on the support so the composites were applied to the central 6096 mm (20 ft.). Stiffness tests were again performed on the new span lengths and those results are used in the comparisons for strength and stiffness.

The two specimens chosen were girders 1 and 2. The corrosion of specimen 1 was significantly worse than that of specimen 2. However, the same amount of composite material was used on both based on using the field evaluation to size the composites and applying the same rehabilitation to all the girders. Girder 1 was repaired at the University of Delaware while girder 2 was repaired at the ATLSS laboratory, simulating on-site procedure. The rehabilitation procedure for the two

girders was similar except that girder 2 was in an overhead position with the tension flange down, as would be the case for a field rehabilitation. The inside and outside of each tension flange was sandblasted to remove the oxide layer. This revealed an extremely pitted and non-uniform surface. Each beam was wiped with a solvent prior to bonding. The same carbon pultrusions used in rehabilitation scheme five were chosen to repair the girders. The pultruded strips were cut to 6096 mm lengths. Each strip was sandblasted with a portable unit on-site and cleaned with a solvent. The two-part epoxy was mixed (Figure 5) and applied to the surface of the girder (Figure 6) and to the surface of the carbon strips (Figure 7). The 6096 mm assemblies of composite strips were lifted into place by hand (Figure 8) and fastened to the steel girder by means of C-clamps and wood tabs (Figures 9 and 10). The composite strips were successfully clamped to the beams within the working time of the epoxy. The adhesive was allowed to set at room temperature for the required 24 hours. The feasibility of using heating methods to increase the curing rate of the adhesive was demonstrated by using both heating blankets and induction heaters to elevate the temperature in the member at discrete locations. The elevated temperatures were monitored with infra-red equipment.

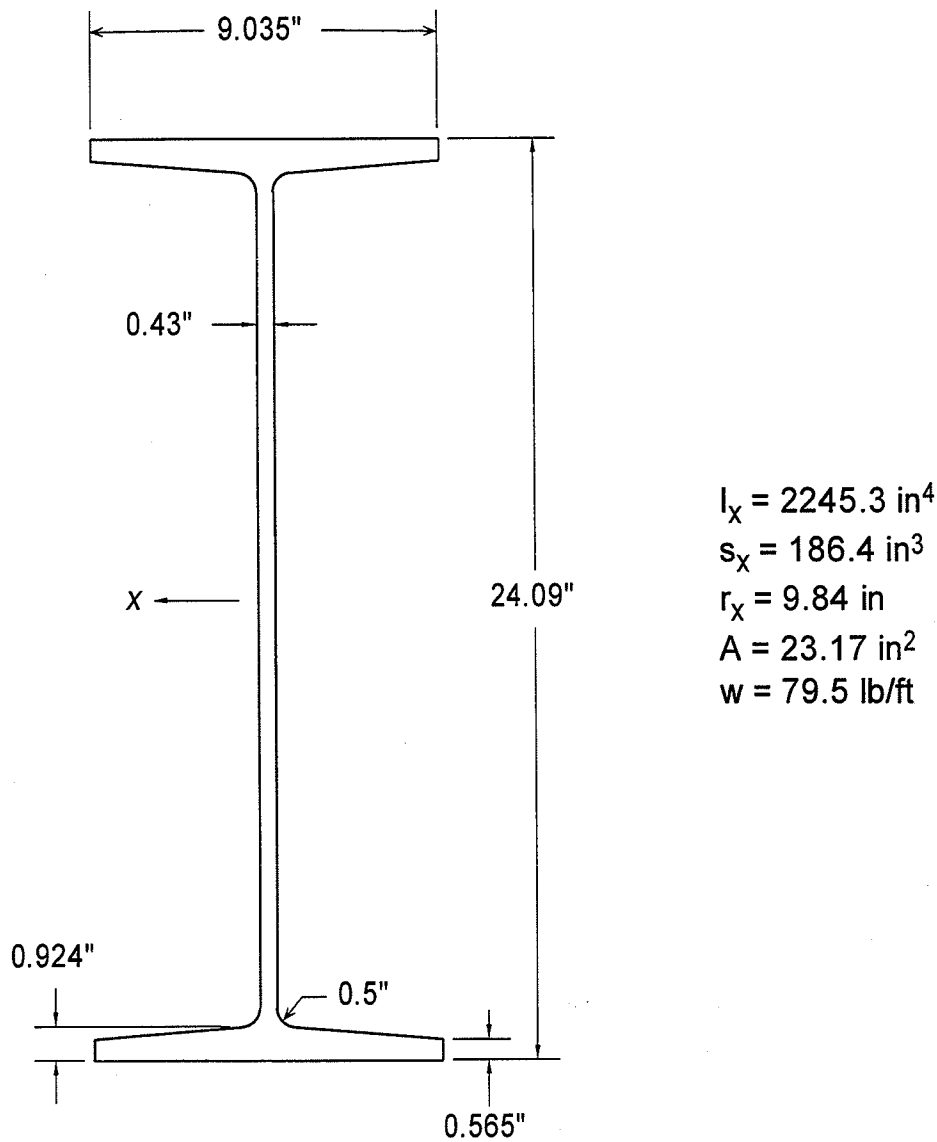


FIGURE 4 Original section.



FIGURE 5 Mixing epoxy.

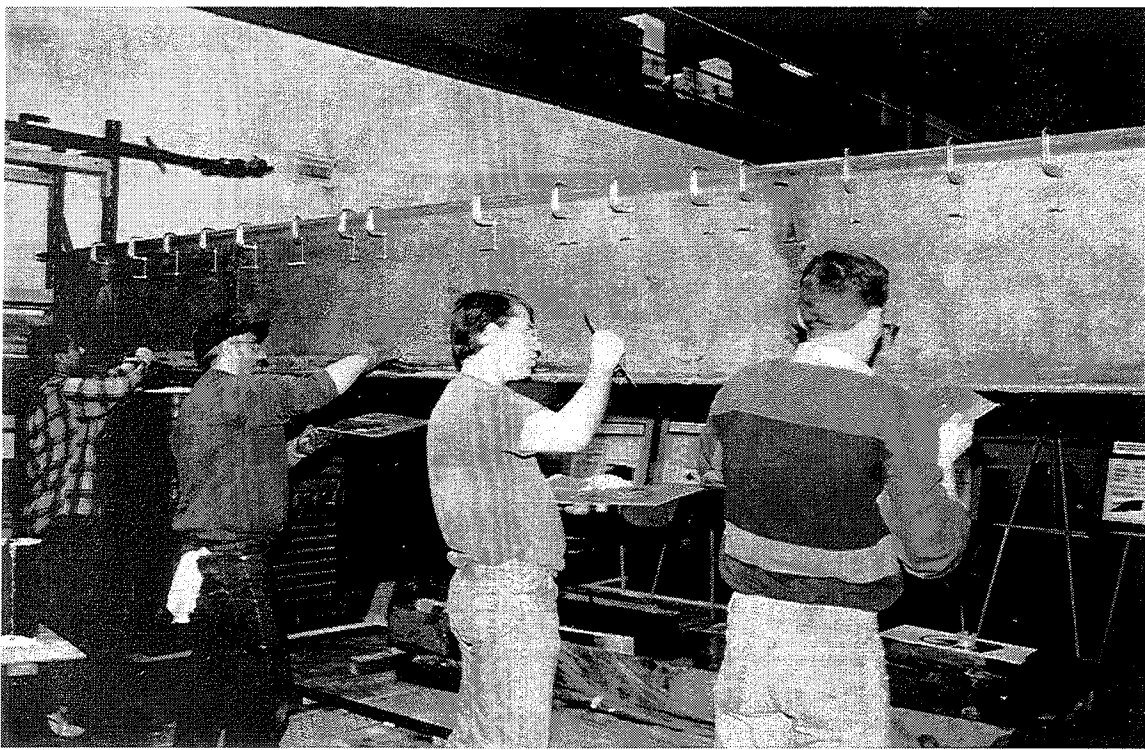


FIGURE 6 Application of epoxy to girder surface.

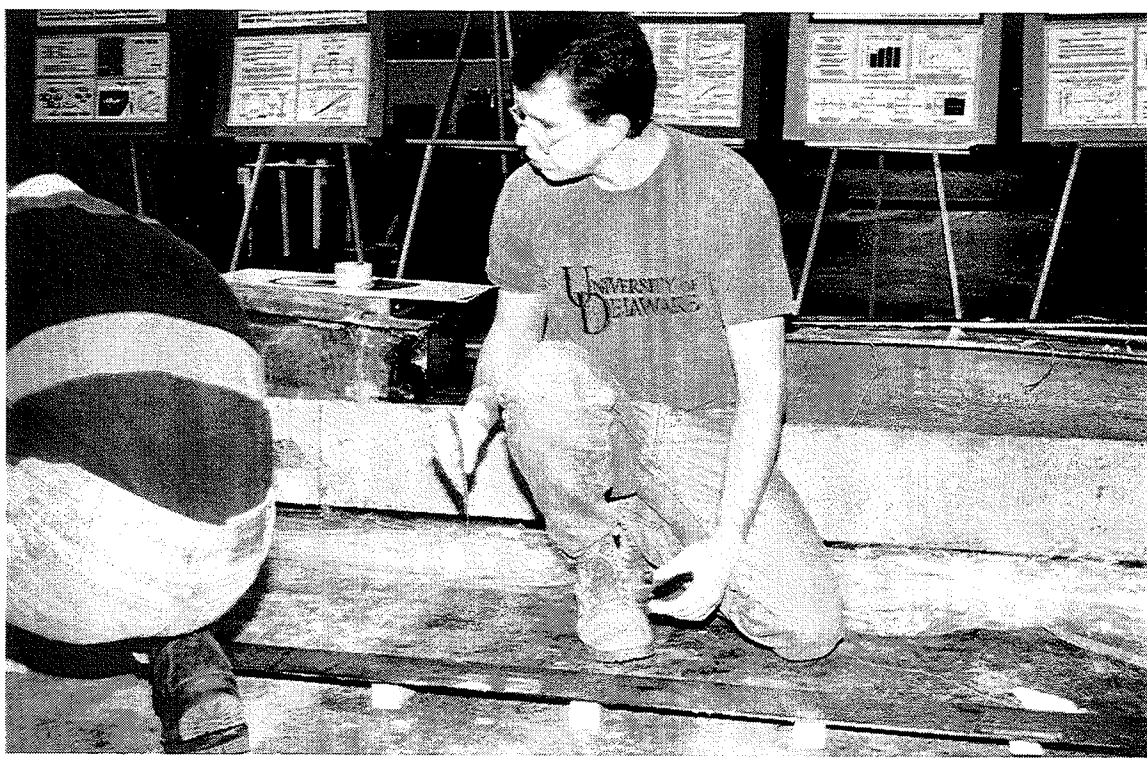


FIGURE 7 Application of epoxy to pultruded carbon composite strips.

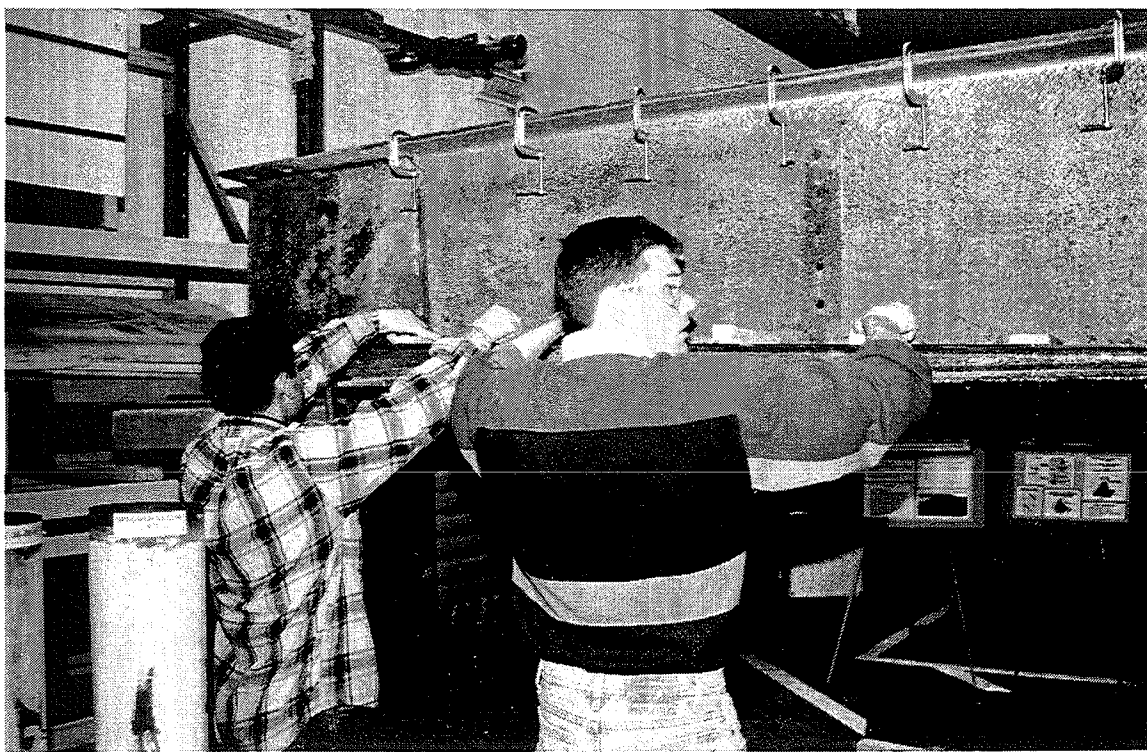


FIGURE 8 Manual placement of rehabilitation.

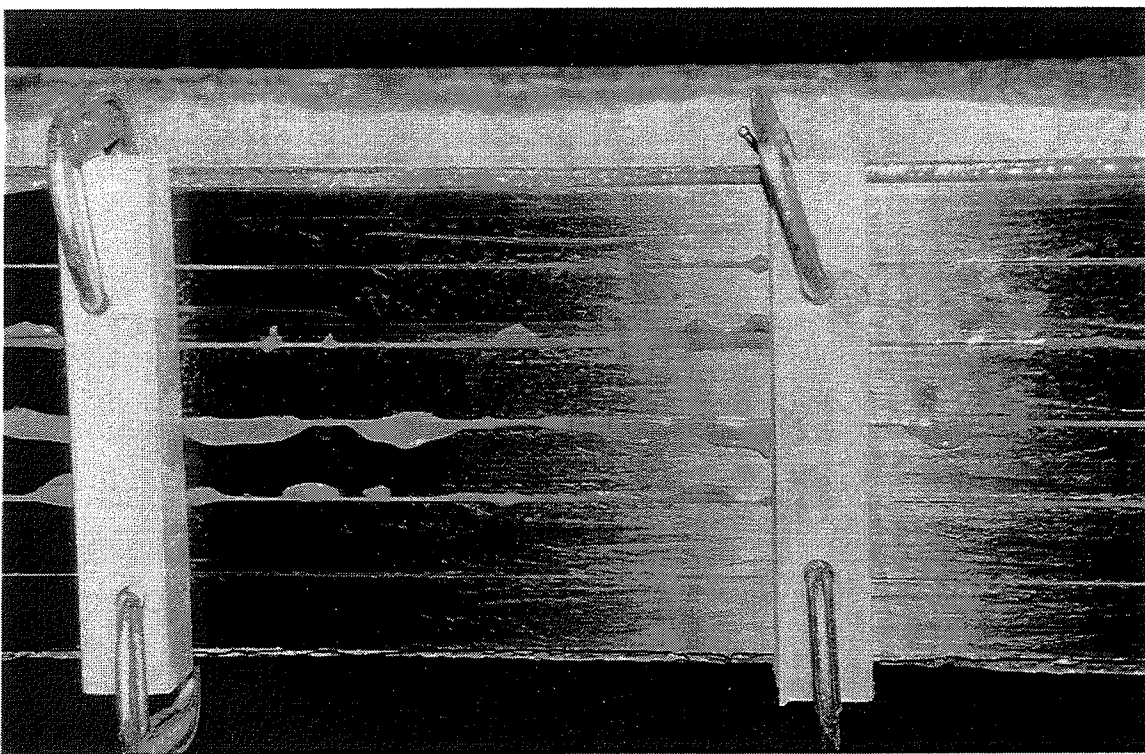


FIGURE 9 Rehabilitated girder: bottom flange view.

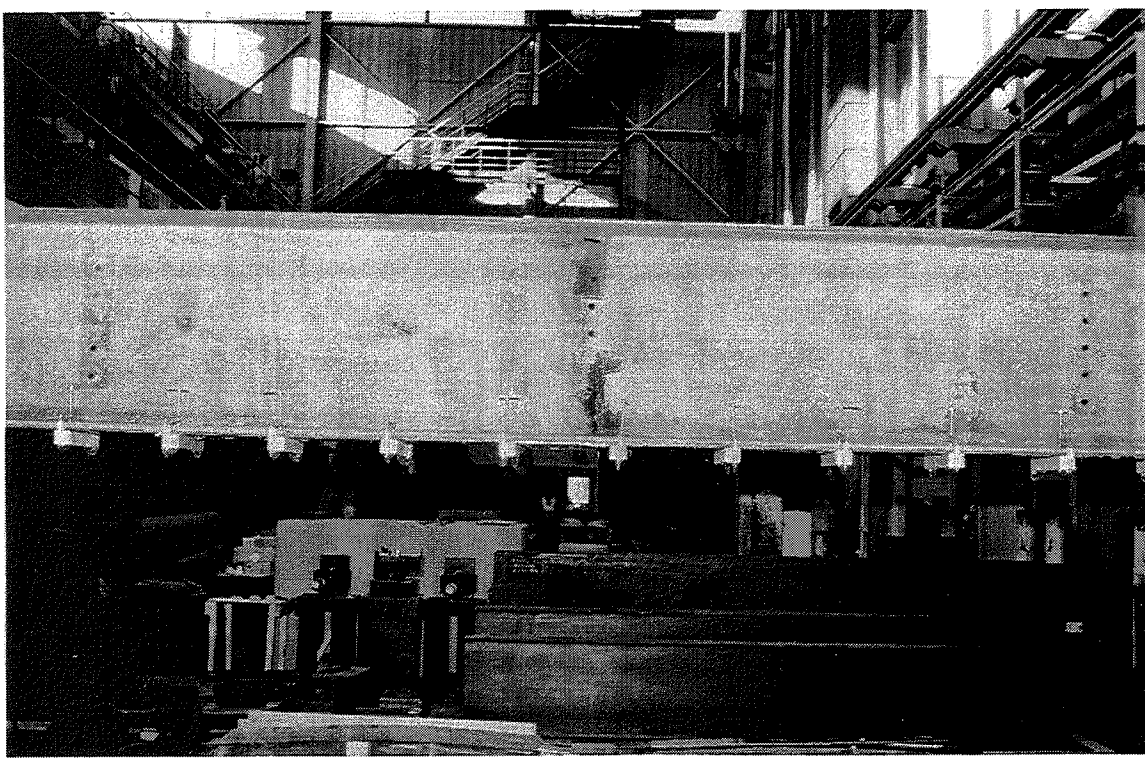


FIGURE 10 Rehabilitated girder: side view.

Post-Repair Ultimate Testing

Test Setup

After the on-site repair procedure was completed and bearing stiffeners were installed in the two test girders at the ATLSS laboratory, they were shipped to Fritz laboratory where the ultimate tests were performed. Consistent with the elastic tests at the University of Delaware, the test span was 6401 mm (21 ft.) for both tests. The tests were executed in the 22,240 kN (5 million lbs.) Baldwin universal testing machine. A drawing and picture of the test setup are shown in Figures 11 and 12, respectively. The girders were laterally braced at the supports, near the third points, and on either side of the load point. The load was applied through a 152 mm (6 in.) roller under the machine head. The girders were supported at the ends on 152 mm (6 in.) rollers.

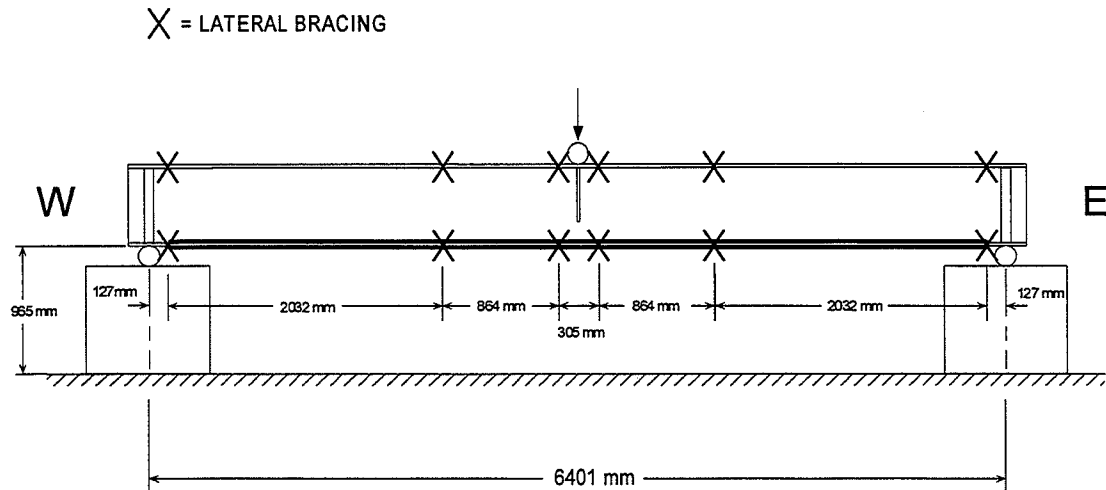


FIGURE 11 Test setup.

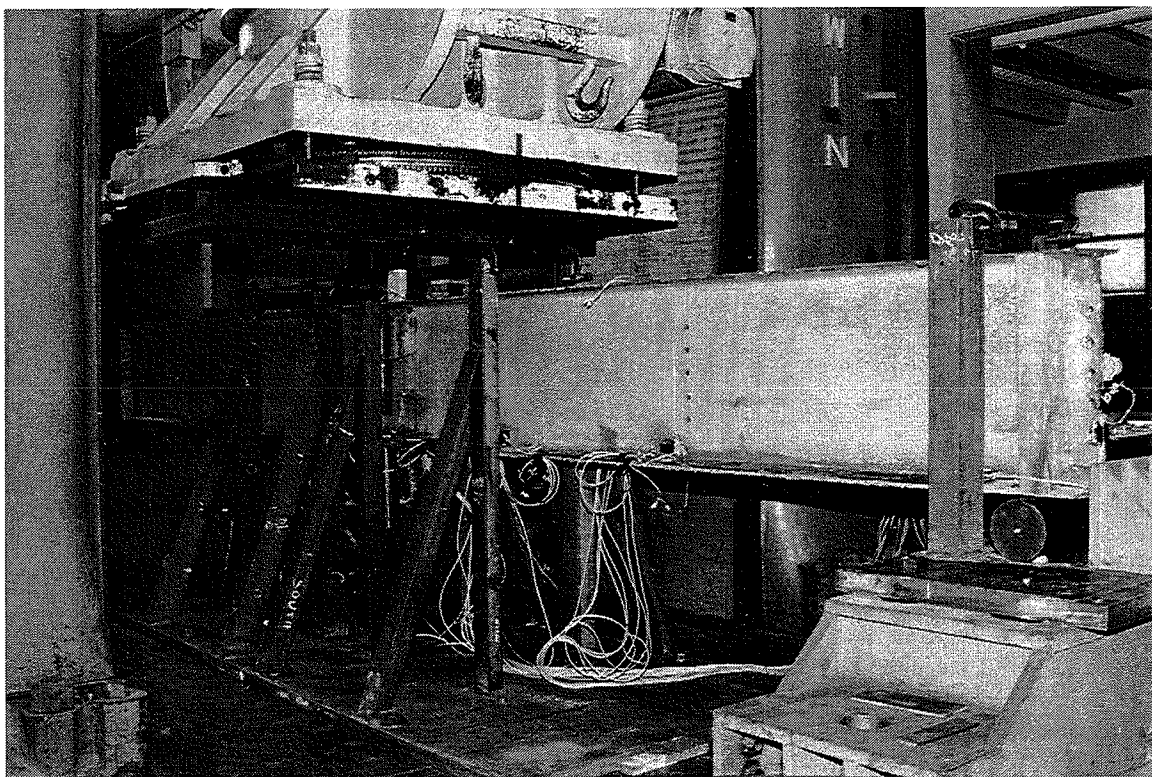


FIGURE 12 Photograph of test.

Instrumentation

An extensive instrumentation plan was developed in order to determine both the global and local behavior of the retrofitted girders. Strain gages were mounted at three sections on the girder, located 152 mm (6 in.), 914 mm (3 ft.), and 1829 mm (6 ft.) from the centerline of the section. At each section, gages were placed at various locations through the depth on both the steel and composite. Figure 13 contains drawings of the strain gage locations. In addition to the strain gages, various voltage devices were used. A displacement transducer was used to measure the centerline displacement of the girder. Displacement transducers were also used at the girder ends to measure any relative slip between the composite strips and the beam flange, as this was the failure mode in the small-scale tests. Clinometers were installed to measure the rotations of the beam at the end, and 914 mm (3 ft.) on either side of centerline. The location of all voltage devices is illustrated in Figure 14.

Test Procedure

The test procedure was monotonic, that is one loading direction until failure. Initially, each girder was elastically cycled up to 222 kN (50 kip) and back. After two cycles, the girders were loaded until failure. The test machine ran under pseudo-load-control. A slow loading rate was maintained throughout each experiment. The total duration of each experiment was approximately 2 hours per specimen.

Test Results

Figure 15 contains the load-displacement relationship for the two specimens. As is shown, both the stiffness and strength of the badly corroded girder 1 were less than those of girder 2. Both specimens exhibited very ductile behavior, however their load carrying capacity was limited by local buckling of the top flange (Figure 16). The composite material on girder 1 never reached its ultimate state even after large deformation, and the test was halted due to damage occurring in the lateral bracing. For the second test, damage to the lateral bracing was no longer a concern so girder 2 was loaded to even larger displacements in an effort to break the composite material. As seen in Figure 15, the girder underwent large inelastic deformation.

Table 6 summarizes the stiffness of the two girders pre- and post-repair. The FEA predictions were in close agreement with the experimentally determined stiffness changes. Table 7 contains the strength comparisons for the two specimens. This shows the effectiveness of composite repair. Note that the ultimate strength of both specimens was governed by the local buckling limit state. If this could be prevented, the strength increases would have been even greater, as was determined by the FEA and the simplified analysis method. The predictions for the member in its original state, corroded state, and repaired state according to the FEA are shown in Figure 17.

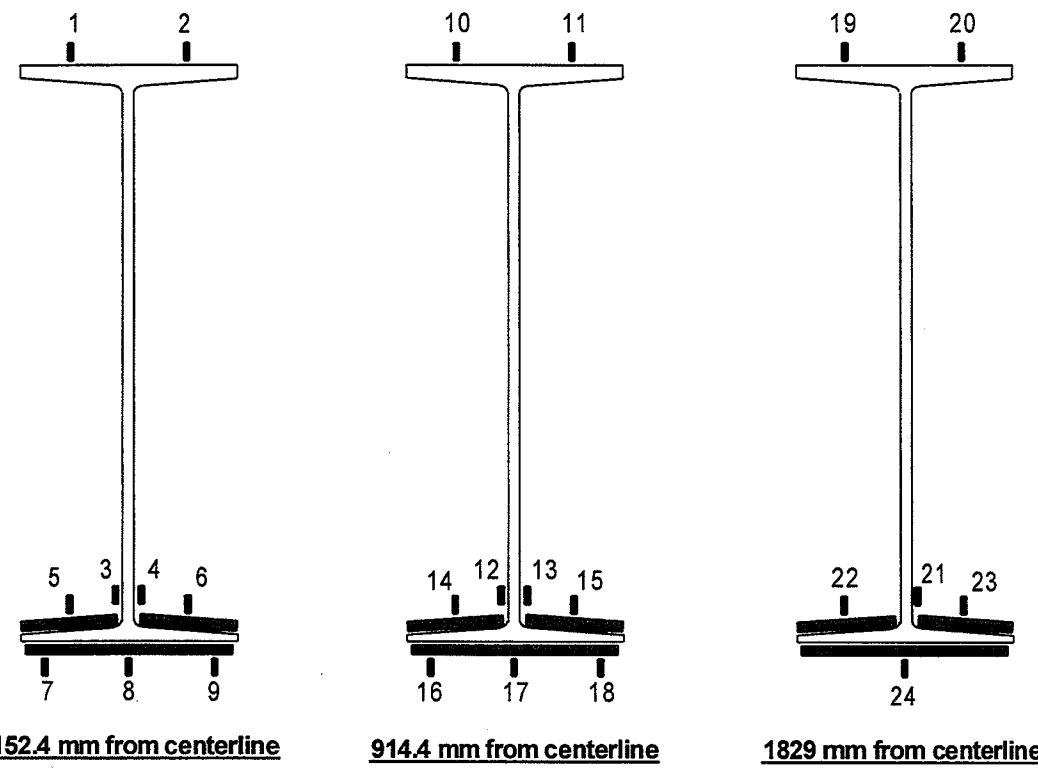
TABLE 6 Elastic Stiffness Comparison

		Elastic Stiffness, k (kN/mm)	% of Original
Original Stiffness (new girder):		32.8	
Girder 1	Unrepaired	20.5	62 %
	Repaired	27.4	83 %
Girder 2	Unrepaired	28.5	87 %
	Repaired	32.0	97 %

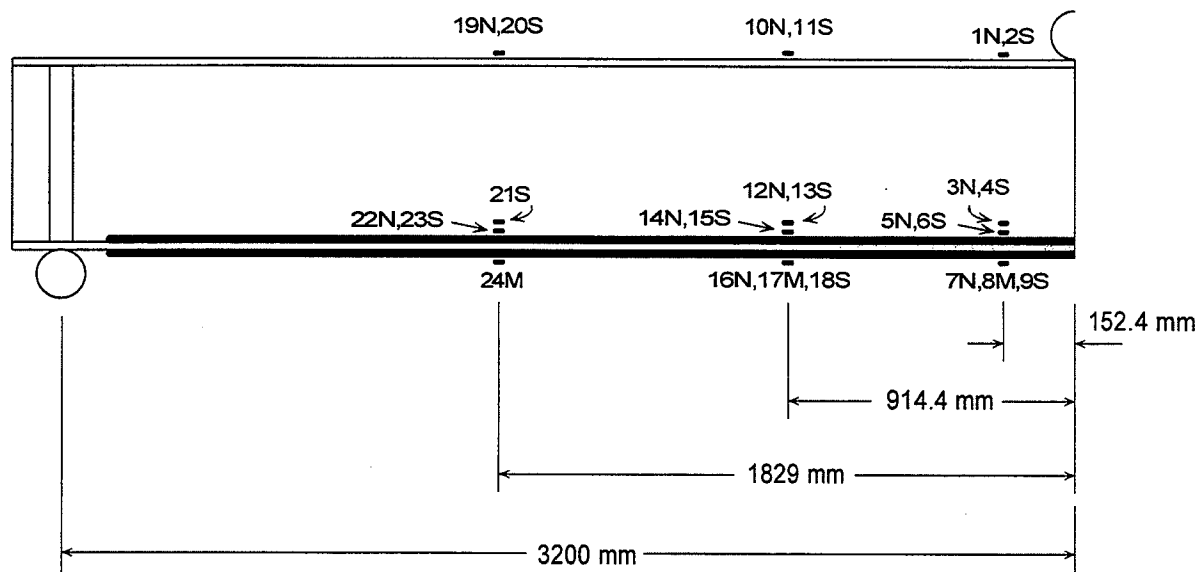
TABLE 7 Strength Comparison

		Maximum Moment (kN-m)	% of Original
Original Plastic Moment (new girder)		$M_p = 994.5$	
Girder #1	Unrepaired	$M_p = 679.9^*$	68 %
	Repaired	$M_{max} = 842.1$	85 %
Girder #2	Unrepaired	$M_p = 879.9^*$	88 %
	Repaired	$M_{max} = 1119.0$	113 %

* M_p of unrepaired section based on FEA



(a)



(b)

FIGURE 13 Strain gage locations.

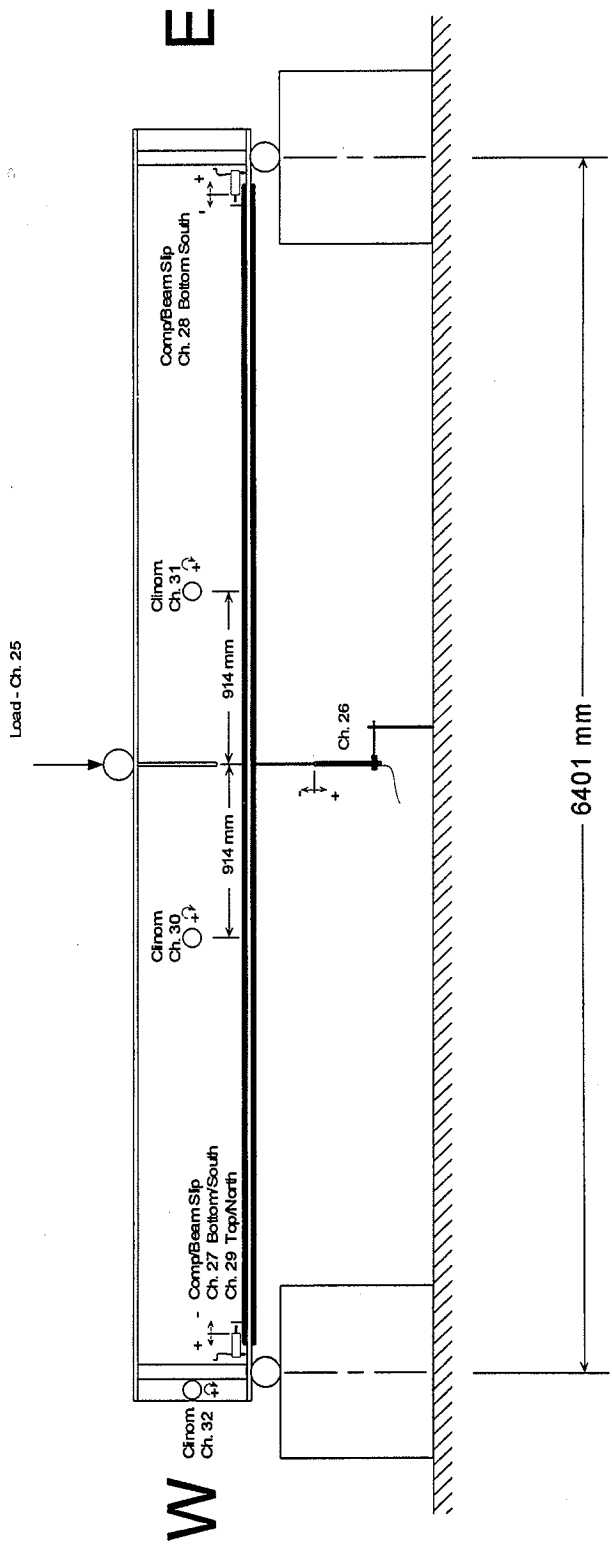


FIGURE 14 Voltage device locations.

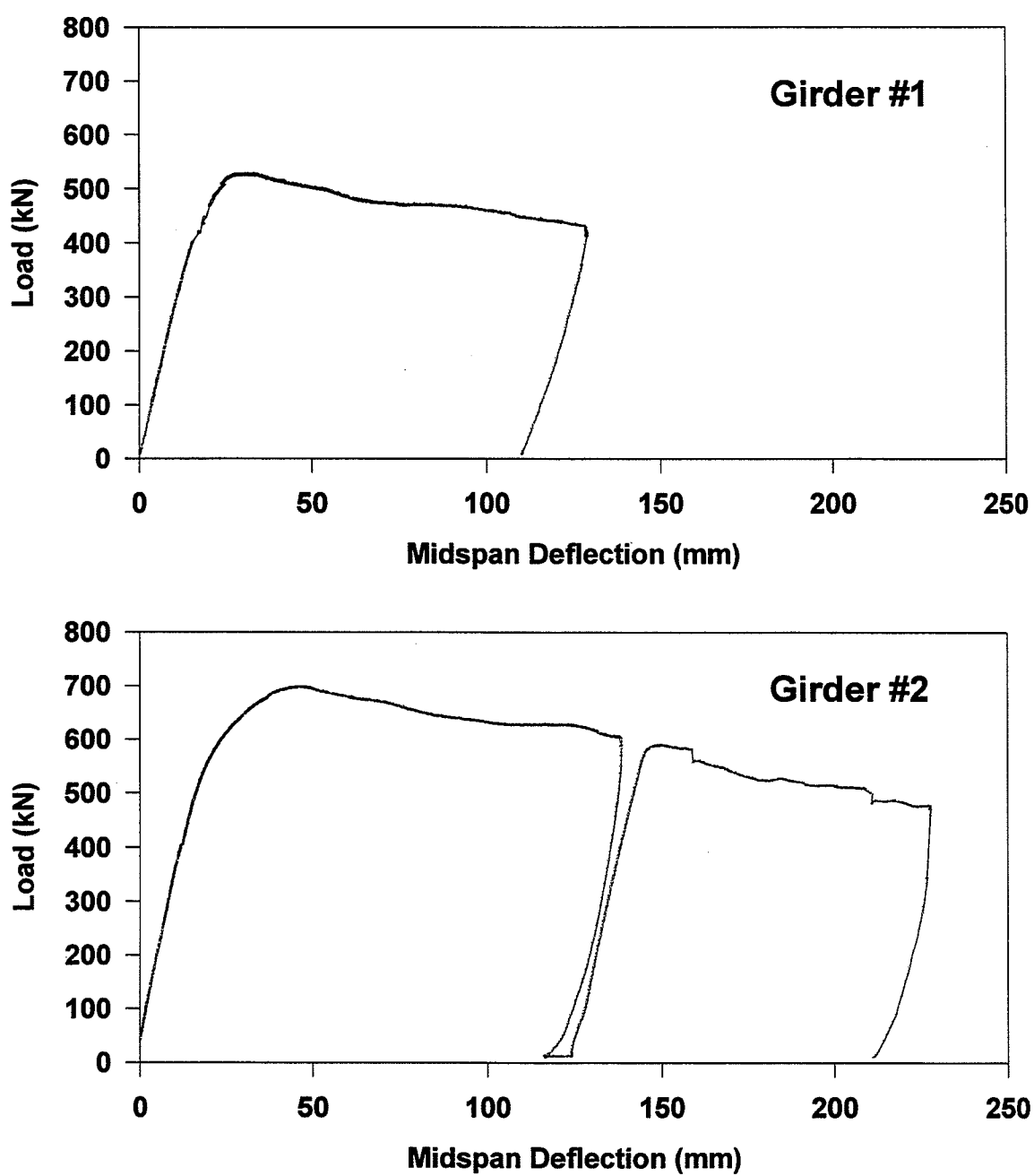


FIGURE 15 Load-deflection curves for girder 1 and girder 2.

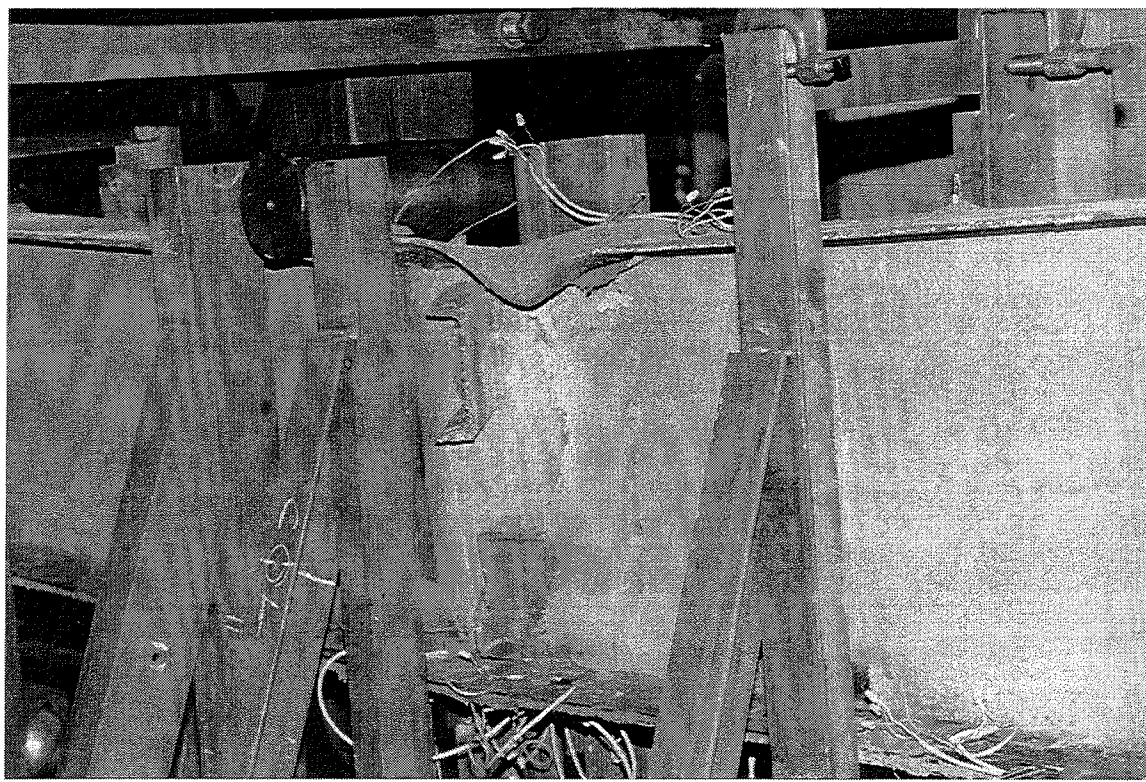


FIGURE 16 Local buckling of top flange.

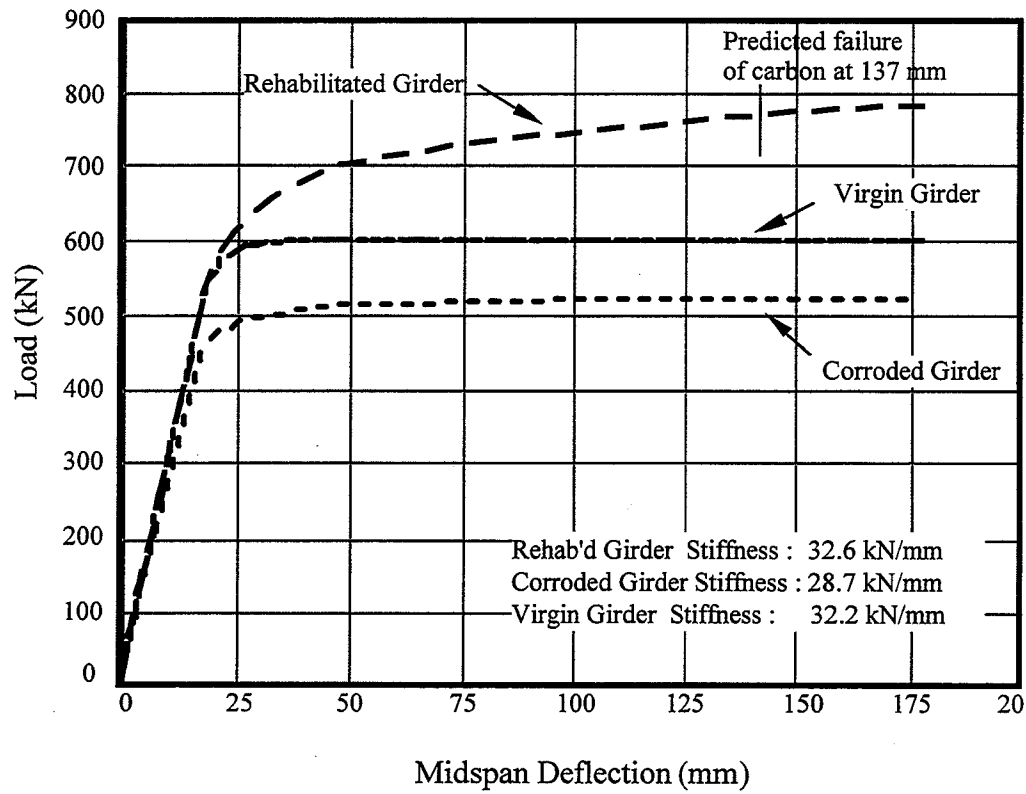


FIGURE 17 FEA predictions.

The displacement transducers mounted at the ends of both girders indicated that no significant relative slipping occurred between steel and composite. Figures 18–21 show the load-strain histories prior to the onset of flange buckling for both specimens at the two sections closest and farthest from the loading point of the beam. At the section closest to the load point (Figures 18 and 20), the unreinforced top flange developed significant inelastic strain. However, the reinforced bottom flange was kept to a much lower strain level; the composite was still elastic and helped to control the growth of inelastic strains in the steel. At the section 1829 mm from the loading point (Figures 19 and 21), the strains remained proportional to the applied load as no yielding occurred at this location.

Plots of the neutral axis location versus applied load for the two specimens can be seen in Figures 22 and 23. In general, the neutral axis significantly shifted towards the reinforced tension flange when steel yielding occurred. The neutral axis shifted less in the case of the weaker girder 1; once the comparatively smaller bottom flange yielded, higher resistance from the composite was required to satisfy equilibrium. This resulted in higher strain demand on the composite which corresponds to a higher neutral axis compared with the stronger girder 2.

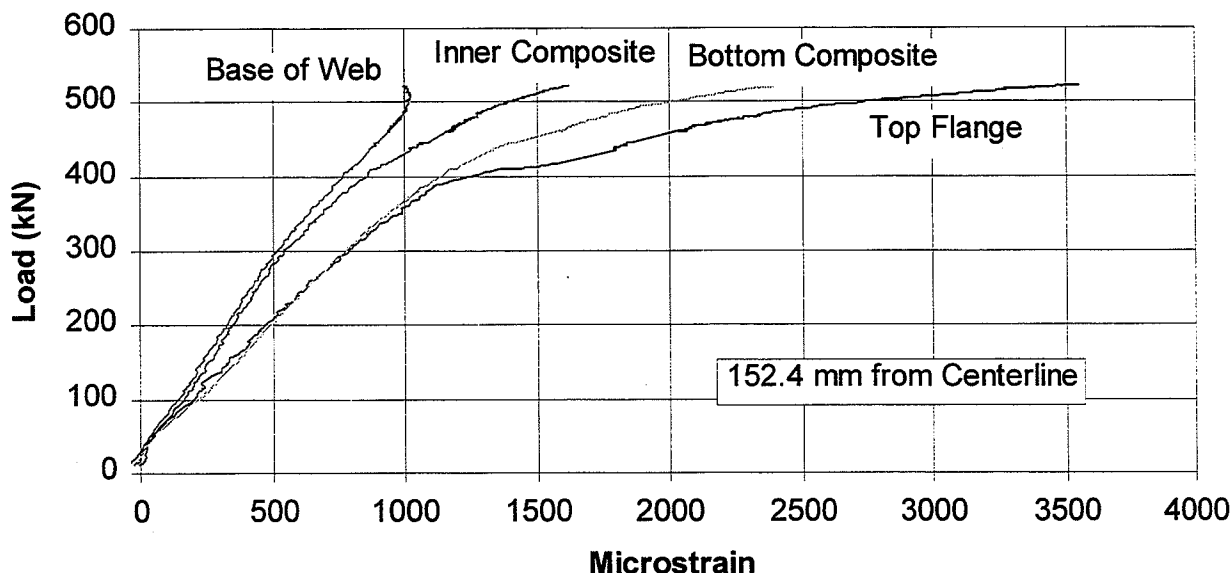


FIGURE 18 Girder 1: Load vs. strain 152.4 mm from centerline.

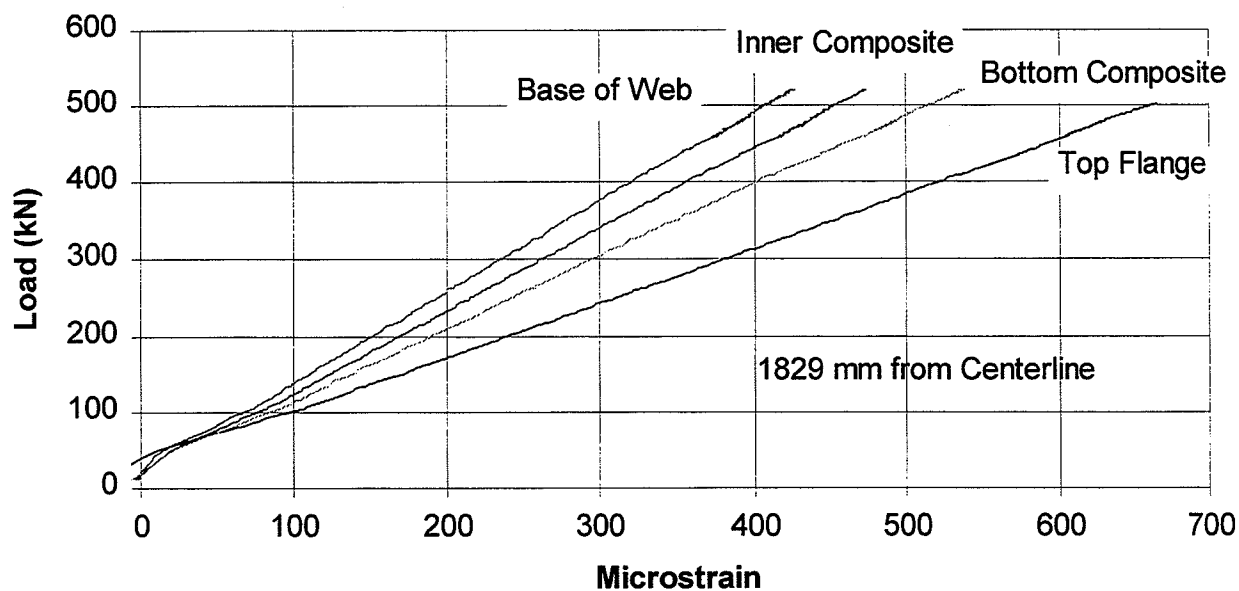


FIGURE 19 Girder 1: Load vs. strain 1829 mm from centerline.

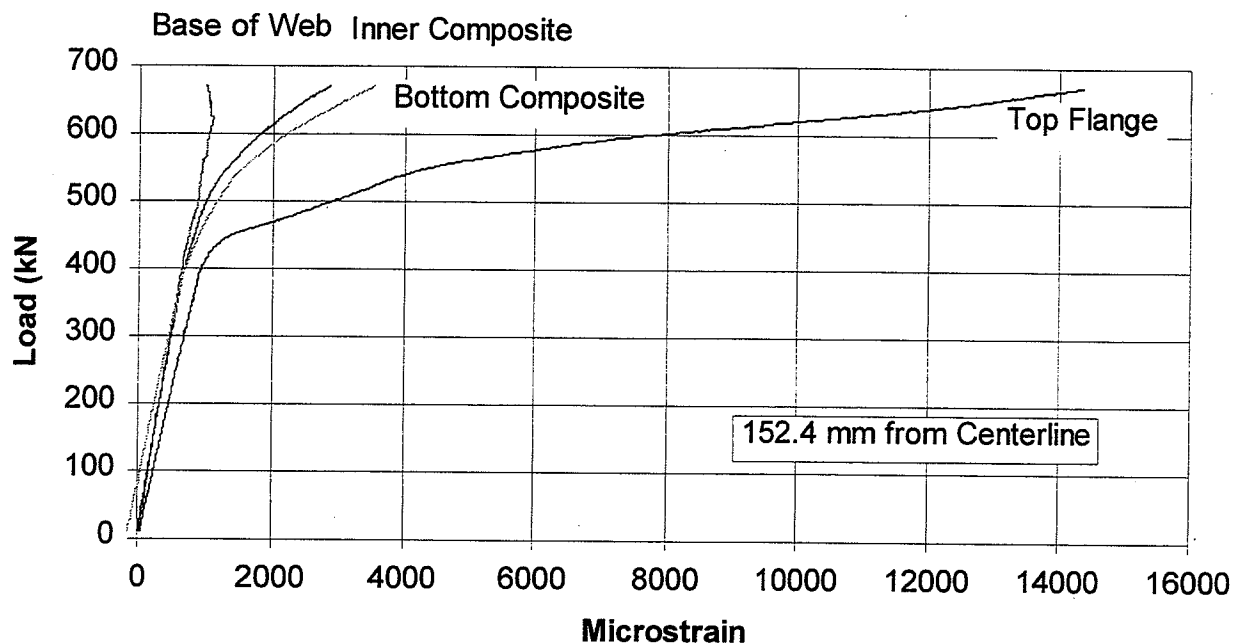


FIGURE 20 Girder 2: Load vs. strain 152.4 mm from centerline.

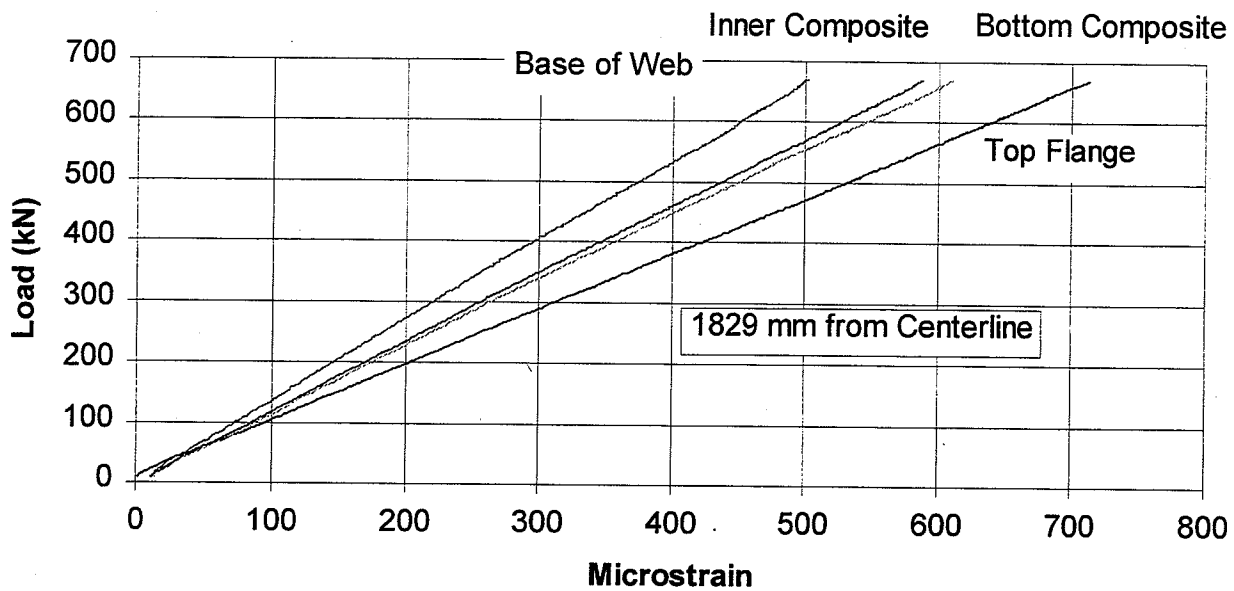


FIGURE 21 Girder 2: Load vs. strain 1829 mm from centerline.

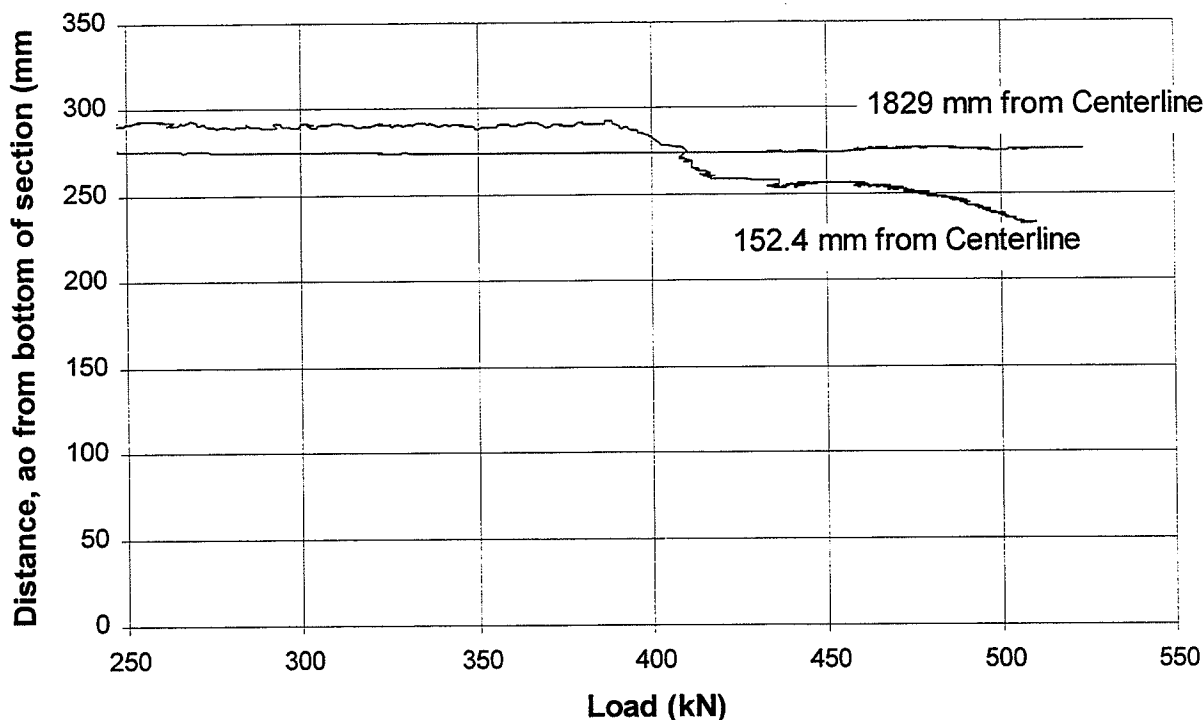


FIGURE 22 Girder 1: Neutral axis location vs. load.

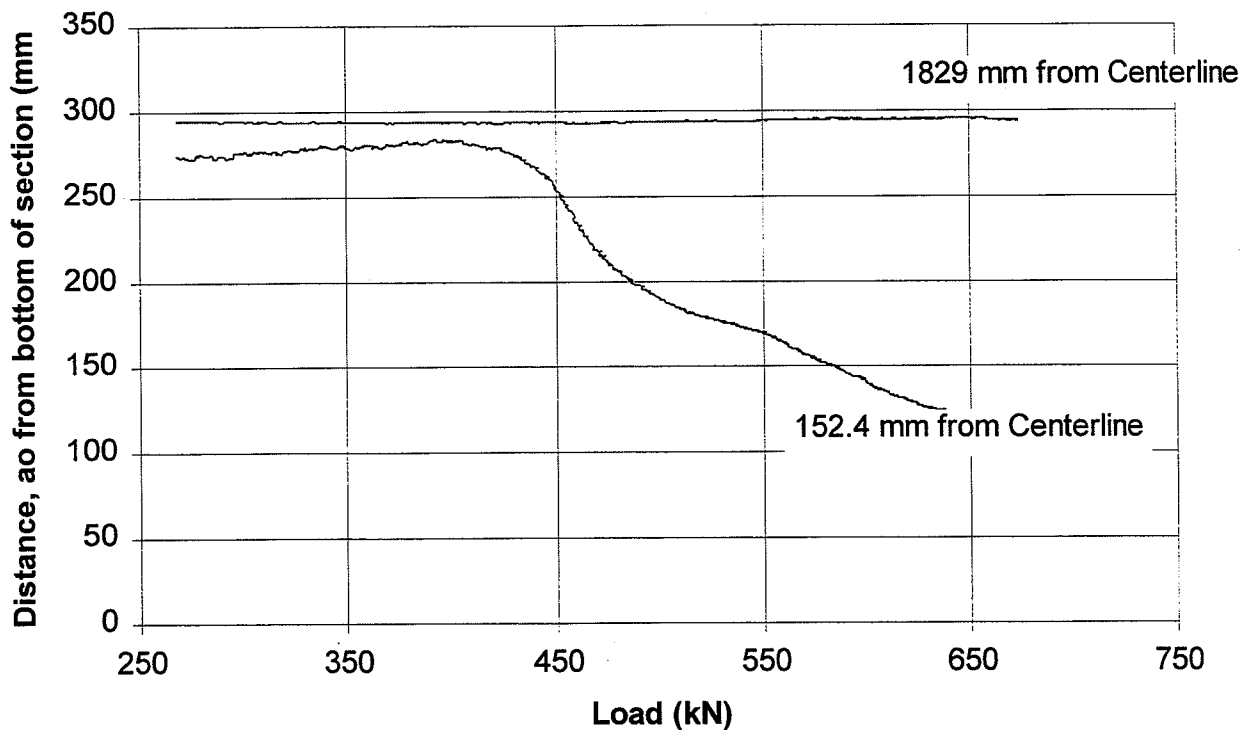


FIGURE 23 Girder 2: Neutral axis location vs. load.

Simplified Analysis Method

Analytical Method

A simplified nonlinear analysis method was formulated to capture the load-deformation behavior of the steel girder having the bottom flange repaired with the bonded composite material. A concrete slab on top of the girder can be included in the analytical model. The purpose of this development was to provide a simplified analytical tool that could be used to design and evaluate the stiffness, strength, and ductility of the repaired girder. In contrast to the sophisticated three-dimensional finite element analysis, the method is a modification of a conventional beam analysis.

The model for the cross-section of the repaired beam consists of steel section, composite sections, and concrete slab. We make the following assumptions:

1. The repaired girder is subjected to 3-point loading as applied in our experiments;
2. The steel material has elastic-perfectly-plastic stress-strain relationship;
3. The concrete material is effective only under compression, and has non-linear stress-strain relationship;
4. The composite material develops essentially elastic response, and;
5. Deformations of all the above materials are assumed to be fully compatible, maintaining a plane cross-section.

The cross-section model consists of 34 segments for the repaired girder with slab model. Eight segments are used for the concrete and two for the composite material. The stress-strain relationship for each segment is assigned depending on the material used. The following summarizes the analysis procedures:

For a given bottom fiber strain, the location of the neutral axis is obtained by satisfying equilibrium, compatibility, and the linear or non-linear stress-strain relationship of the segments. The moment and curvature corresponding to this strain distribution can then be obtained. The entire moment-curvature relationship of the section is then obtained by successively incrementing the bottom fiber strain, obtaining the moment and curvature each time. For a given center load, the distribution of bending moment along the span is obtained. By performing double integration of the corresponding curvature distribution with respect to span direction, we obtain the deformation of the girder. The computation is repeated by increasing the magnitude of the load, and thus the load-deformation of the repaired girder is obtained. An interactive microcomputer program "SECTION" is developed to carry out the calculation, and its FORTRAN source code and sample input file are listed in Appendix A.

Correlative Analysis

The repaired girder 1 discussed earlier is analyzed using the SECTION program. The analytical model uses the dimensions as well as material properties determined previously. A concrete slab was not attached in the experiment, thus, its effect is not considered.

Figure 24 plots the experimentally- and analytically-obtained load-displacement curves for girder 1. The analysis accurately predicts both elastic and inelastic behavior of the repaired girder in the pre-buckling stage. The analysis does not consider the compression flange buckling, thus its prediction at the post-buckling range is not reliable. However, if the experiment had included a concrete slab, the buckling could have been avoided. Based on this, the analysis method would be reasonably accurate for a presumably typical case where flange buckling is not present.

Analytical Evaluations for Repair Effectiveness

Using the program, the following cases were analyzed:

1. Unrepaired girder without slab.
2. Repaired girder without slab.
3. Unrepaired girder with 203-mm-thick (8 in.) slab on top.
4. Repaired girder with 203-mm-thick (8 in.) slab on top.

Figure 25 plots the predicted load versus displacement for each of the cases. Note that all analyses were ended when the bottom fiber strain reached 8,000 microstrain. When the slab is not present, the stiffness, yield strength, and ultimate strength of the repaired girder are about 1.2, 1.2, and 1.5 times those of the unrepairs girder. Analysis indicates about 76 mm (3 in.) deflection before composite strain reaches the ultimate 8,000 microstrain. Also, the composite material helps to reduce the inelastic tension strains of the steel at the bottom flange region. For the same deflection, the strain of repaired girder is about 0.5 times that of the unrepairs girder.

The repair effect becomes more prominent when the slab on top of the girder is considered: the stiffness, yield strength, and ultimate strength of the repaired girder are about 1.2, 1.3, and 2.0 times those of the unrepairs girder. Significant increase of the ultimate strength is due to the upward shifting of the beam neutral axis. Shifting occurs due to stiff performance of the compressed slab region, which makes the contribution of the composite more significant. This indicates the importance of including the concrete slab in an evaluation of the composite repair scheme.

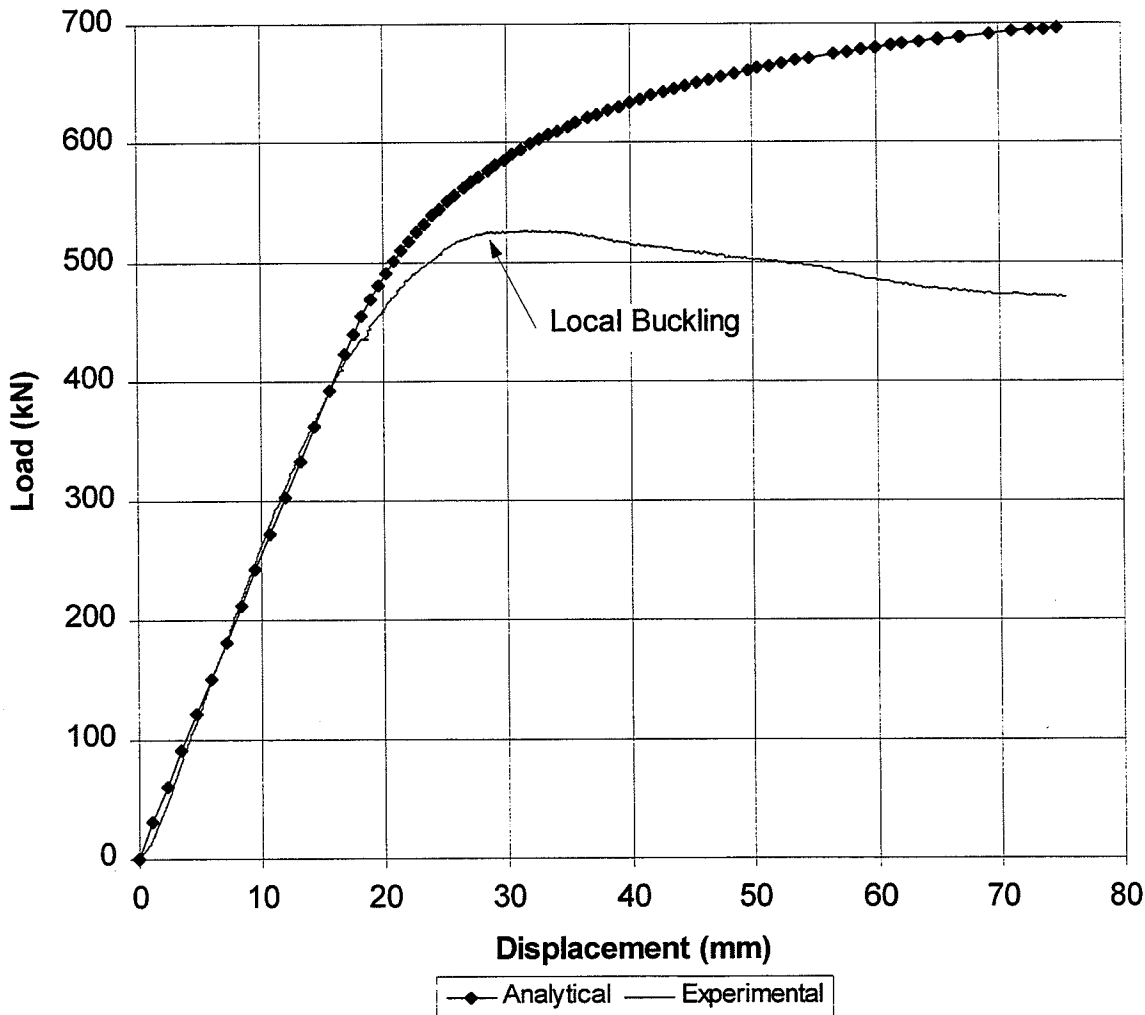


FIGURE 24 Girder 1: Analytic and experimental load-deflection curves.

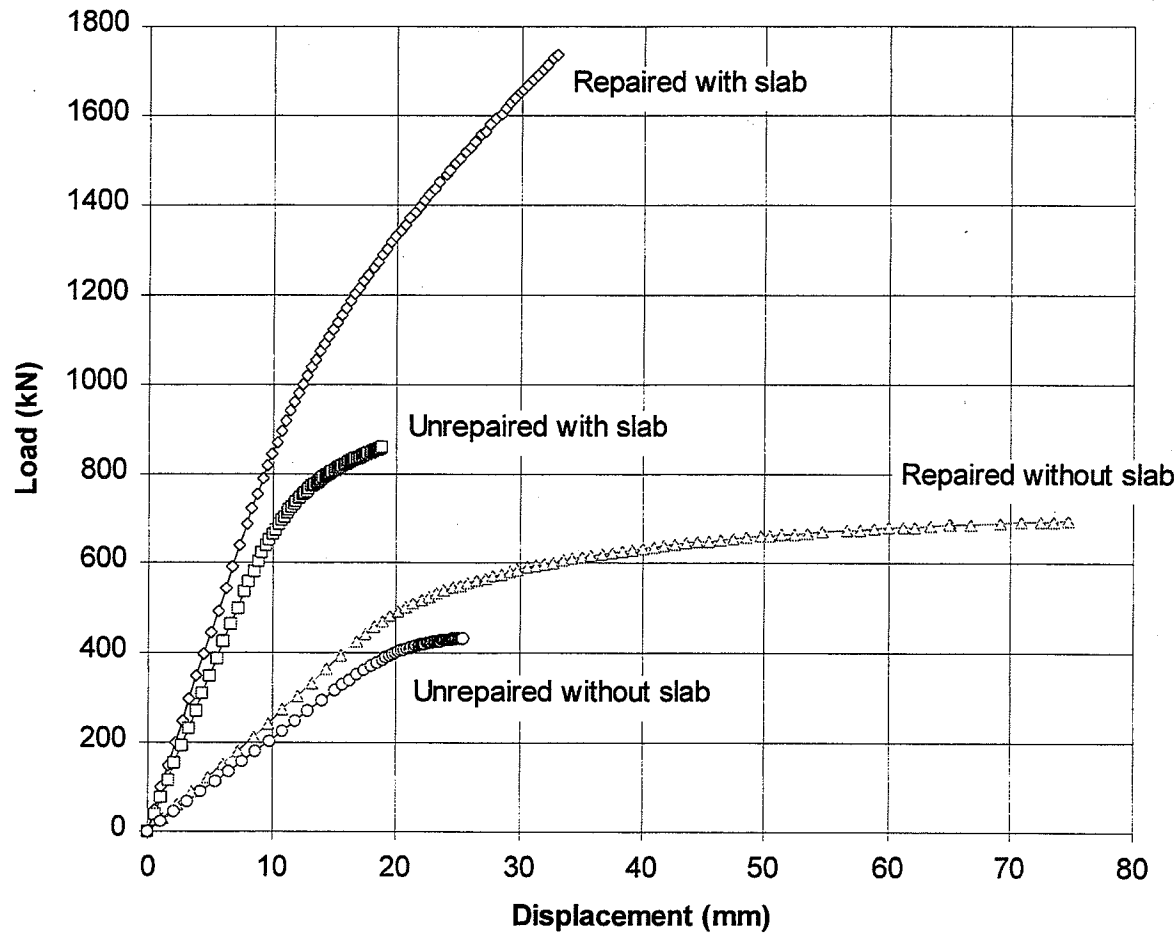


FIGURE 25 Multi-case comparison using simplified analysis method.

CONCLUSIONS

Strength and stiffness increases were significant. The strength of the girders could have been larger had local buckling been prevented, which is typical of the case in which a concrete slab is present on the top flange. Analysis of the severely corroded girder 1 with the current composite size shows a 25% increase in stiffness and a 100% increase in strength. Furthermore, better performance could be achieved through the use of larger composite elements, provided an adequate bond is present.

Experimental results indicate that the inelastic strains in the steel tension flange were significantly reduced by the composite material which was confirmed through our simplified analysis method. Moreover, the analysis for the same girder with a typical concrete slab indicated even greater reductions. Inelastic strains were reduced to only 0.25 times the unreinforced case at the same load level, indicating significant benefit of composite repair in protecting overload in the tension flange.

Elastic strains were reduced to 0.8 times the unreinforced case showing the capacity of the composite for improving the fatigue life of the steel. Since fatigue life has a logarithmic relationship with strain range, the fatigue life can increase to 4 times under such an amount of strain reduction. Furthermore, if this decrease is below the endurance limit strain, then fatigue life is no longer a concern. These benefits can be magnified further if larger composite elements are attached to the tension flange. These conclusions are contingent on a sufficient fatigue life of the composite as well as the adhesive.

Designing a composite rehabilitation consists of determining the geometry best suited to the situation, evaluating the current stiffness losses due to corrosion, choosing a composite material, and sizing the rehabilitation to restore the lost stiffness to an acceptable level. The next step is to examine the elastic strength of the new section, the ultimate failure mechanism that will govern, and determine the load at which that failure will occur. For one of the small beams tested, failure occurred due to bond failure at a load lower than the elastic strength. This failure is undesirable and should be prevented in the design process. To maximize the potential of the composite materials, the most desirable failure mode is to cause the fibers in the composite to be broken at the location of maximum moment. This results in the largest amount of ductility and the largest increase in ultimate strength over elastic strength. This is analogous to achieving the plastic moment capacity in a compact, braced steel girder. Other failure mechanisms that can occur before this optimal state include the failure mechanisms typical to a bridge girder and some failure modes specific to the composite rehabilitation.

The failure modes typical to a bridge girder consist of lateral torsional buckling (not a problem for slab-on-girder type bridges), local buckling of either the compression flange or the web (not a problem for slab-on-girder compact members), and loss of the connection from the steel girder to the concrete slab.

The premature failure mode of greatest concern with the bonded composites is failure of the adhesive bond. This failure occurs due to concentrations of shear and peeling stresses acting at the termination of the composite patch. This mode was prevalent in the small tests conducted where shear forces were large relative to bending forces and large curvatures were present at the termination of the composite. This failure mode was absent from the large girder tests where the span length caused shear forces to be small relative to bending forces and large curvatures were concentrated at the midpoint. The effect on bridges in the field acting composite with concrete decks is expected to fall between these two extremes. The key to preventing this failure mode in cases where shear stresses and curvatures will be large at the termination of the composite is to taper the composite over a sufficient length. Therefore, for certain span lengths, this failure mode will not be an issue, while tapering will be necessary for shorter spans.

Another concern is in regard to Poisson ratio mismatches between the composite materials and the steel, which can cause edge failures. This problem is readily solved by using composites laminates with Poisson ratios in the primary to secondary direction that are similar to that of steel; this ratio will usually be similar for unidirectional composites which are recommended for applications where the surface variability does not require the use of a fabric rehabilitation.

The future corrosion of the base steel member should not be accelerated by the composite rehabilitation. Galvanic corrosion can occur between the carbon fibers in a composite material and the steel. To avoid this problem, a layer of E-glass material should be inserted between the carbon composite and the steel girder. This layer will electrically insulate the two materials from each other and prevent galvanic corrosion.

Finally, durability of the composite rehabilitation must be ensured by employing an adhesive that will resist environmental attack. Some qualified adhesives were discussed previously.

In view of the above conclusions, future research should include testing of specimens including a concrete slab, as well as fatigue loading. Further, retrofit with different sizes and configurations of composite materials should be investigated. It is our impression that the composite repair method addressed in this report is a promising solution to steel bridge girder rehabilitation.

APPENDIX A

PROGRAM SECTION

```
*****
* This program calculates the moment-curvature relationship for a given section.
* The properties of the section are input from a data file. The section is
* discretized, and location, area, modulus of elasticity, and yield stress
* are given for each discrete segment in consistent units.
* Concrete segments can be input by inputting location, area, fc', and a
* flag that defines the section as being concrete. This flag is 1 if the
* section is concrete and 0 for all other sections.
* A non-linear stress-strain curve for concrete in flexure is used for the
* concrete segments. The curve was developed by Hognestad and is given in
* Figure 15.2.1 of Wang and Salmon, "Reinforced Concrete Design 5th ed."
* Then, given the span length, the program calculates the load-deflection
* relationship by integrating the curvature twice over the length of the span.
* This assumes a 3-pt. bending configuration with the load applied at
* centerline.
*
* NOTE: The first segment should be either the topmost or bottommost segment
* An initial guess for the neutral axis should be given in the input
* file.
*
* Programmed by Ian C. Hodgson April 10, 1996
*
*** Important Variables ***
*
* X() - Locations of segments (input)
* A() - Areas of segments (input)
* E() - Moduli of segments (input)
* FY() - Yield strength of segments (input)
* STRAIN() - Strain in segments
* C - distance from 1st segment to neutral axis
* F() - Force in segments
* TOL - c tolerance (input)
* STRINC - 1st segment strain increment (input)
* MNT() - Moment at each strain increment
* C0, C1, C2 - Coefficients in force equilibrium eqn. used to calculate c
* SPAN - Span length (input)
* THETA() - Rotations at increments along beam length
* DELTA() - Displacements at increments along beam length
* PHI() - Curvatures at increments along beam length
* THETAO - Rotation at support (maximum)
* DELTA0 - Displacement at support (maximum, disp. at midspan is taken as 0 for
* easier numerical integration)
* NUMSEC - Number of segments in section (input)
* NUMINC - Number of strain increments (input)
* STR0() - Shown in Figure 15.2.1 Wang & Salmon
* FC() - fc' for each segment (input)
* CONCR() - flag indicating whether segment is concrete or not (input)
*
```

```
REAL X(256),A(256),E(256),FY(256),STRAIN(256),C,F(256)
+ ,TOL,STRINC,MNT(256),C0,C1,C2,CNEW,SPAN,THETA(256)
+ ,DELTA(256),PHI(256),THETAO,DELTA0,STR0(256),FC(256)
INTEGER NUMSEC,NUMINC,CONCR(256)
CHARACTER*12 INPF,OUTF
```

```
WRITE(*,*)' * Enter input filename *'
READ(*,'(A)')INPF
WRITE(*,*)' * Enter output filename *'
READ(*,'(A)')OUTF
```

```
OPEN(9,FILE=INPF)
```

```
READ(9,*)NUMSEC
```

* Data is read from the input file

```
DO 10 I=1,NUMSEC
READ(9,*)X(I),A(I),E(I),FY(I),CONCR(I)
10 CONTINUE
```

```
READ(9,*)C,TOL,STRINC,NUMINC
READ(9,*)SPAN
```

```
OPEN(10,FILE=OUTF)
```

```
WRITE(10,1001)'Moment,Rot.,Strain(1),c,Phi,Load,Disp.,Sum F'
```

```
1001 FORMAT(1X,A45)
```

```
WRITE(*,*)" ... Working ... "
```

```
STRAIN(1)=0
DO 12 J=1,NUMINC
MNT(J)=0
12 CONTINUE
```

```
DO 13 I=1,NUMSEC
IF(CONCR(I).EQ.1)THEN
  FC(I)=FY(I)/1000.
  E(I)=(1800000.+500*0.85*FC(I)*1000.)/1000.
  STRO(I)==-2*0.85*FC(I)/E(I)
END IF
13 CONTINUE
```

* This is the outermost loop. Each time the program calculates all quantities
 * for a given strain in the 1st segment.

```
DO 40 INC=1,NUMINC
STRAIN(1)=INC*STRINC
```

* Within this nested loop, the program calculates the force in each segment, and
 * the coefficients C0, C1, & C2 from the force equilibrium equation. Then the
 * distance to the neutral axis, C is the solution of the quadratic eqn,
 * $C0*c^2 + C1*c + C2 = 0$.
 * This is repeated. If the difference between the two values of c are within
 * the tolerance, the program continues.

```
15 C0=0
C1=0
C2=0
```

```
DO 20 I=1,NUMSEC
STRAIN(I)=STRAIN(1)*(1-X(I)/C)
IF (CONCR(I).EQ.0)THEN
  IF (ABS(STRAIN(I)).LT.(FY(I)/E(I)))THEN
    F(I)=A(I)*STRAIN(I)*E(I)
    C0=C0+STRAIN(I)*A(I)*E(I)
    C1=C1-STRAIN(I)*A(I)*E(I)*X(I)
  ELSE
    F(I)=A(I)*FY(I)*STRAIN(I)/ABS(STRAIN(I))
    C0=C0+F(I)
  END IF
ELSE
  IF (STRAIN(I).GT.0)THEN
    F(I)=0
  ELSE IF (STRAIN(I).GT.STRO(I))THEN
```

```

28      F(I)=-A(I)*0.85*FC(I)*(2*STRAIN(I)/STRO(I)-(STRAIN(I)/
+           STRO(I))**2)
+           C0=C0-(2*A(I)*0.85*FC(I)*STRAIN(1)/STRO(I)-A(I)*0.85*
+           FC(I)*STRAIN(1)**2/STRO(I)**2)
+           C1=C1-2*A(I)*0.85*FC(I)*(STRAIN(1)**2/STRO(I)**2*X(I)-
+           STRAIN(1)/STRO(I)*X(I))
+           C2=C2+A(I)*0.85*FC(I)*STRAIN(1)**2/STRO(I)**2*X(I)**2
ELSE IF (STRAIN(I).LT.-0.0038)THEN
    WRITE(*,*)'*** Concrete crushed at segment',I,' ***'
    WRITE(10,*)'*** Concrete crushed at segment',I,' ***'
    WRITE(10,*)'STRAIN = ',STRAIN(I)
    GO TO 50
ELSE
    F(I)=A(I)*(-0.15*0.85*FC(I)/(0.0038-STRO(I))*(
        (STRAIN(I)+STRO(I))-0.85*FC(I)))
    C0=C0+A(I)*(-0.15*0.85*FC(I)/(0.0038-STRO(I))*(
        (STRAIN(1)+STRO(I))-0.85*FC(I)))
    C1=C1+A(I)*(0.15*0.85*FC(I)*X(I)*STRAIN(1)/
        (0.0038-STRO(I)))
END IF
END IF

20 CONTINUE

CNEW=(-C1+SQRT(C1**2-4*C0*C2))/(2*C0)

IF(ABS(CNEW-C).GT.TOL)THEN
    C=CNEW
    GO TO 15
END IF

TOTFORCE=0

* The moment is calculated by summing the forces in each segment times the
* distances to the segments.

DO 30 I=1,NUMSEC
    MNT(INC)=MNT(INC)-F(I)*X(I)
    TOTFORCE=TOTFORCE+F(I)
30 CONTINUE

* The curvature equals the strain at the bottom segment divided by the distance
* to the neutral axis.

PHI(INC)=STRAIN(1)/C

* If the program is past the 2nd strain increment, it calculates the rotations
* and displacements of the beam when the current strain distribution occurs at
* centerline.
* Instead of discretizing the beam uniformly, it uses the past values of Phi,
* and knowing that the moment diagram for a 3-pt. bend is always linear (it is
* statically determinate), the moment can be used to calculate the distance
* along the beam where the curvature corresponding to that moment occurs. In
* other words, the distance along the beam and the moment in the beam are
* proportional.

IF(INC.GT.2) THEN

    THETA(INC)=0

* Within this loop, the program calculates the rotations in the beam, assuming 0
* rotation at the center of the beam. The trapezoidal rule is used.
* Integration starts from the center and proceeds to the support, which is

```

```

* analogous to a cantilever beam.

      DO 35 K=INC-1,1,-1
          THETA(K)=(PHI(K+1)+PHI(K))/2*(MNT(K+1)-MNT(K))*SPAN/
          + (2*MNT(INC))+THETA(K+1)
35 CONTINUE

      THETA0=PHI(1)/2*MNT(1)*SPAN/(2*MNT(INC))+THETA(1)

      DELTA(INC)=0

* Here the displacements are determined using the trapezoidal rule. A
* displacement of 0 is assigned at the load point (cantilever)

      DO 36 K=INC-1,1,-1
          DELTA(K)=(THETA(K+1)+THETA(K))/2*(MNT(K+1)-MNT(K))*SPAN/
          + (2*MNT(INC))+DELTA(K+1)
36 CONTINUE

      DELTA0=(THETA(1)+THETA0)/2*MNT(1)*SPAN/(2*MNT(INC))+DELTA(1)

      END IF

      WRITE(10,1010)MNT(INC),2*DELTA0/SPAN,STRAIN(1),C,PHI(INC),
      + MNT(INC)*4/SPAN,DELTA0,TOTFORCE

1010 FORMAT(1X,8(E12.5,','))

      40 CONTINUE

      50 WRITE(*,*)"... Done ..."

      STOP
      END

```

Number of Segments

0,1.806,16400,1000,0
 0.18,1.35,29000,40.3,0
 0.33,1.35,29000,40.3,0
 0.51,1.806,16400,1000,0
 0.98375,0.497725,29000,45.6,0
 2.14125,0.497725,29000,45.6,0
 3.29875,0.497725,29000,45.6,0
 4.45625,0.497725,29000,45.6,0
 5.61375,0.497725,29000,45.6,0
 6.77125,0.497725,29000,45.6,0
 7.92875,0.497725,29000,45.6,0
 9.08625,0.497725,29000,45.6,0
 10.24375,0.497725,29000,45.6,0
 11.40125,0.497725,29000,45.6,0
 12.55875,0.497725,29000,45.6,0
 13.71625,0.497725,29000,45.6,0
 14.87375,0.497725,29000,45.6,0
 16.03125,0.497725,29000,45.6,0
 17.18875,0.497725,29000,45.6,0
 18.34625,0.497725,29000,45.6,0
 19.50375,0.497725,29000,45.6,0
 20.66125,0.497725,29000,45.6,0
 21.81875,0.497725,29000,45.6,0
 22.97625,0.497725,29000,45.6,0
 23.6925,2.475,29000,40.3,0
 23.9675,2.475,29000,40.3,0
 24.605,60,4000,4000,1
 25.605,60,4000,4000,1
 26.605,60,4000,4000,1
 27.605,60,4000,4000,1
 28.605,60,4000,4000,1
 29.605,60,4000,4000,1
 30.605,60,4000,4000,1
 31.605,60,4000,4000,1

12.0,0.0075,100E-6,80
 252.0

Individual Segment Data

$x_i, A_i, E_i, F_{yi}, 0$

for elastic-perfectly-plastic segments

$x_i, A_i, f'_c, f_c, 1$

for concrete segments

$c_{initial}, c_{tolerance}, \epsilon_{inc}, \# inc$
span length

(note: c is the x coordinate of the neutral axis)

GIRDER#1 with 8" slab with 60" effective width; $f'_c=4000$

SAMPLE INPUT FILE